Feeding ecology and habitat use of the reef manta ray (*Mobula alfredi*) in the Chagos Marine Protected Area, Indian Ocean revealed using stable isotope analysis

by

Geneviève Alexander

Thesis submitted to Plymouth University in partial fulfilment of the requirements for the degree of

MRes Marine Biology

Plymouth University

Faculty of Science & Engineering

September 2022

Journal format: *Ecology and Evolution*

Masters Dissertation licence

This material has been deposited in the Plymouth University Learning & Teaching repository under the terms of the student contract between the students and the Faculty of Science & Technology.

The material may be used for internal use only to support learning and teaching.

Materials will not be published outside of the University and any breaches of this licence will be dealt with following the appropriate University policies.

ABSTRACT

Effective conservation of threatened species relies on identification of key habitats, such as those used for foraging. The reef manta ray (*Mobula alfredi*) is a threatened species of planktivorous elasmobranch in rapid global decline due to targeted fishing and incidental bycatch. A local population of *M. alfredi* reside in the Chagos Archipelago, central Indian Ocean. The archipelago is encompassed by a 640,000 km^2 no-take Marine Protected Area (MPA), however Illegal, Unreported and Unregulated (IUU) fishing remains a prevalent issue and continue to target elasmobranchs as a high value catch. Here, we use stable isotope analysis of $\delta^{13}C$ and $\delta^{15}N$ of *M. alfredi* muscle and skin tissue to investigate the feeding ecology and habitat use of this local population within the MPA. 70 bulk plankton samples and 41 *M. alfredi* tissue biopsies were collected from various locations within the MPA and analysed to calculate their isotopic signatures of $\delta^{13}C$ and $\delta^{15}N$. Isotopic values of $\delta^{13}C$ of *M. alfredi* skin displayed a depletion of $\delta^{13}C$ in 2019, suggesting a variation in foraging location which coincides with the extreme positive Indian Ocean Dipole event and fluctuating plankton availability. Bayesian mixing models estimate Egmont Lagoon and Peros Banhos as likely foraging hotspots (20-25% of diet input) for both skin and muscle tissue, suggesting that *M. alfredi* feed in these locations on a seasonal and annual basis. Peros Banhos is an atoll with relatively few *M. alfredi* sightings and the possibility of Peros Banhos as a foraging hotspot provides reason for increased survey effort in this area of the region. Isotopic signatures of $\delta^{13}C$ and $\delta^{15}N$ are significantly different between muscle and skin, indicating a difference in short-term and long-term feeding ecology and habitat use. An improved knowledge of *M. alfredi* habitat use within the MPA is vital to optimise enforcement patrols of illegal fishing vessels to minimise *M. alfredi* catch.

Key words

Mobula alfredi Stable isotope analysis Feeding ecology Habitat use Chagos MPA

1. INTRODUCTION

1.1 Elasmobranchs

Globally, elasmobranch (sharks, skates, and rays) populations are experiencing rapid population declines, threatened by a multitude of anthropogenic pressures including overfishing, habitat loss, climate change and pollution (Seitz & Poulakis, 2006; Chin *et al.,* 2010; Knip *et al.,* 2010; Dulvy *et al.,* 2017). As of 2021, over 32% of elasmobranch species are threatened with extinction, primarily due to targeted fishing and incidental bycatch (Dulvy *et al.*, 2014, 2021; Jorgensen *et al.*, 2022). Their decline is exacerbated by their conservative life history traits which include low reproductive rates, slow growth, late maturation and, consequently, slow population recovery (Dulvy *et al.*, 2017; Jorgensen *et al.*, 2022). In response, many countries have adopted policies to protect elasmobranchs on national and international scales (Jorgensen *et al.*, 2022). Restrictions and regulations surrounding trade of elasmobranch products including fins, meat, gills and teeth, establishment of Marine Protected Areas (MPAs), enforcement of catch-quotas, and accurate reporting of bycatch are all measures implemented to protect elasmobranchs (Jorgensen *et al.,* 2022). Despite these efforts, restrictions on elasmobranch fishing are often insufficient (Dulvy et al 2017). Catch quotas are often set at levels higher than a population can sustainably withstand and do not take into consideration dynamic seasonal or geographical restrictions (Dulvy et al 2017). In many regions, policy enforcement is minimal and Illegal, Unreported and Unregulated (IUU) fishing of highly valued species contributes to the continued population decline of elasmobranchs (Dulvy et al 2017, Agyeman *et al.,* 2021), even in designated no-take MPAs (Ferretti *et al.,* 2018; Hays *et al.,* 2020). Additionally, adequate protection of elasmobranchs is often hindered by a lack of species-specific ecological knowledge, such as habitat use (Gallagher *et al.,* 2012; Jorgensen *et al.,* 2022). A thorough understanding of the spatial dynamics of a species is vital to understand overlap with fisheries (Jacoby *et al.,* 2020). The logistical difficulties and expense to study threatened or inaccessible species has led to many becoming encompassed in 'one-size-fits-all' management policies that do not necessarily consider their unique ecology or conservation requirements (Dulvy *et al.,* 2017; Jorgensen *et al.,* 2022). *Mobulidae* (manta and devil rays) are a group

of elasmobranchs that experience intense fishing pressure and yet relatively little is understood about their feeding ecology and habitat use (Couturier *et al.,* 2012).

1.2. The Reef Manta Ray, Mobula alfredi

Reef manta rays (*Mobula alfredi*) are large, zooplanktivorous elasmobranchs of the *Mobulidae* family (Figure 1). They inhabit shallow, coastal and oceanic island reefs of the tropical Indian and western Pacific Oceans (Figure 2) (Stevens *et al.*, 2018). Populations of *M. alfredi* are resident to home ranges in fragmented local populations (Stevens *et al.,* 2018), however they are capable of making long-distance journeys in excess of 1,000 km to follow seasonal changes of their plankton prey (Armstrong *et al., 2019;* Peel *et al.,* 2020).

Figure 1: The reef manta ray (*Mobula alfredi*). Taken from The Manta Trust (www.mantatrust.org) © Guy Stevens

Mobula alfredi are frequently observed feeding on pelagic zooplankton within surface waters during the daytime (Peel *et al.,* 2019) and, at night, demersal zooplankton undergo vertical migrations from the seabed towards the surface where *M. alfredi* feed (Couturier *et al.,* 2013). As a coastal reef species, *M. alfredi* experience immense pressures due to their close proximity to human settlements, particularly those which exhibit extensive fishing practices with few regulations (MacNeil *et al.*, 2020). Following decades of exploitation, *M. alfredi* was added to Appendix II of the Convention on International Trade in

Endangered Species (CITES) in 2013 and Appendices I and II of the Convention on the Conservation of Migratory Species (CMS) in 2014 (Lawson *et al.,* 2017).

Distribution map of the Reef Manta Ray *Mobula alfredi*. Darker areas indicate confirmed range; lighter areas indicate expected range.

Figure 2: Map of global *Mobula alfredi* distribution with expected range (light blue) and confirmed ranges (dark blue). Taken from Stevens *et al., (*2018).

However, as a result of ongoing exploitation and continuing population decline, *M. alfredi* is now listed as 'Vulnerable' on the IUCN Red List (Marshall *et al.*, 2019). *Mobula alfredi* fecundity is amongst the lowest of all elasmobranchs and thus their population growth is slow. Females reach sexual maturity at around 15 years of age and give birth to one live pup only once every 2-5 years (Stewart *et al.*, 2018; Stevens *et al.*, 2018). Such a low annual reproductive output puts *M. alfredi* at risk of population decline following even low catch rates in artisanal fisheries (Rohner *et al.,* 2013; Croll *et al.,* 2016, Fernando & Stewart, 2021). Currently, twelve countries specifically target mobulid rays for their gill plates and twenty three countries document mobulid bycatch, predominantly by tuna fishery purse seine nets (Couturier *et al.*, 2012; Croll *et al.*, 2016) (Figure 3A). Moreover, the presence of boats, either for fishing or tourism purposes, puts *M. alfredi* at risk of potentially lethal injuries from collisions with boats (Strike *et al.,* 2022) (Figure 3B). To date, *M. alfredi* are perhaps the best studied species of manta ray due to their residency in coastal areas and, therefore, frequent overlap with scuba divers and snorkellers (Stevens *et al.*, 2018). Additionally, *M. alfredi* make regular visits to 'cleaning stations' to be cleaned of

parasites and algal growth (Stevens *et al.*, 2018). The predictability of such visits to 'cleaning stations' and presence of individually unique ventral markings allow researchers to identify individuals and study the same population over years (Stevens *et al.*, 2018). There are, however, local populations of *M. alfredi* that remain relatively understudied due to the remoteness of their home ranges, such as those found in the Chagos Archipelago in the central Indian Ocean (Andrzejaczek *et al.,* 2020)

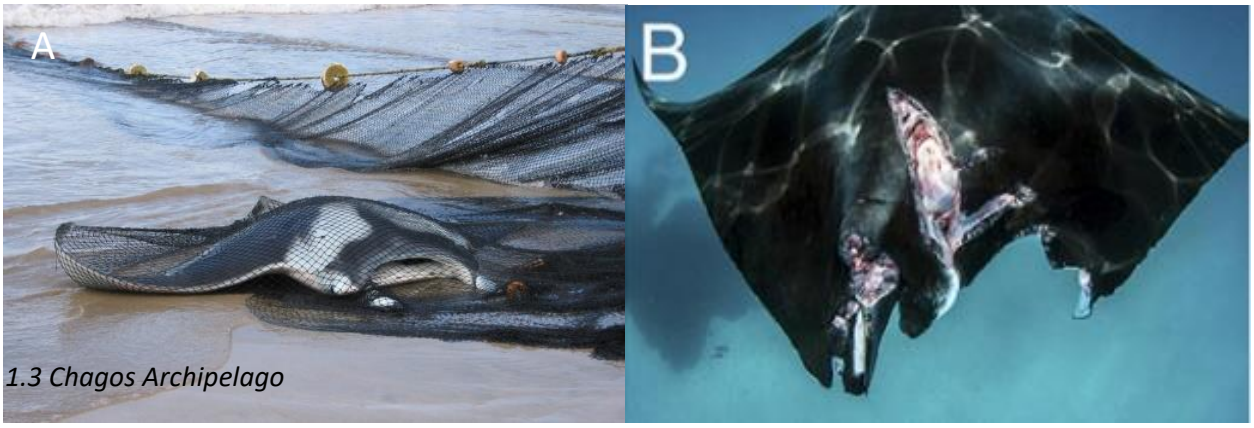

Figure 3: (A) A mobulid caught in a fishing net. Taken from Stevens *et al.,* (2018). (B) A Mobulid with a boat strike injury. Taken from Strike *et al.,* (2022).

The Chagos Archipelago is a collection of seven atolls and sixty low-lying islands in the Indian Ocean, approximately 500 km south of the Maldives (Figure 4). The archipelago has been virtually uninhabited for the last 50 years aside from the presence of a US military base on Diego Garcia in the southeast of the archipelago (Hays *et al.,* 2020). The entire exclusive economic zone (EEZ) of the region is designated as a 640,000 km^2 no-take Marine Protected Area (MPA), one of the largest of its kind in the world (Sheppard *et al.,* 2012). All fishing activity is therefore prohibited, however the MPA is patrolled by a single enforcement vessel which is estimated to detect only 10% of illegal fishing activity (Jacoby *et al.,* 2020) and IUU fishing remains a significant issue within the MPA (Tickler *et al.,* 2019; Collins *et al.,* 2021; Hays *et al.,* 2020).

Aside from the Chagos Archipelago, MPAs in the Indian Ocean are relatively small and dispersed (Marine Conservation Institute, 2021). In the western Indian Ocean, combined MPA area coverage totals 133,273 km^2, covering only 7% of western Indian Ocean continental shelf to varying degrees of protection

(Rocliffe *et al*., 2014). The Chagos MPA, therefore, could be described as a sanctuary within the Indian Ocean for the highly mobile *M. alfredi*. The remoteness of the Chagos MPA and the logistical difficulties of studying *M. alfredi in situ* have limited research opportunities here. Although satellite and acoustic telemetry studies of *M. alfredi* have been carried out to determine movement patterns and habitat use on a regional (Andrzejaczek *et al.,* 2020) and fine scale (Harris *et al.,* 2021), these tagging studies are limited in sample size, spatial range, and temporal scale. In such a remote location, alternative techniques which are not hindered by expensive equipment or labour-intensive methods are favourable, such as stable isotope analysis, (Munroe *et al.,* 2020) and have the potential to reveal *M. alfredi* habitat use across the archipelago.

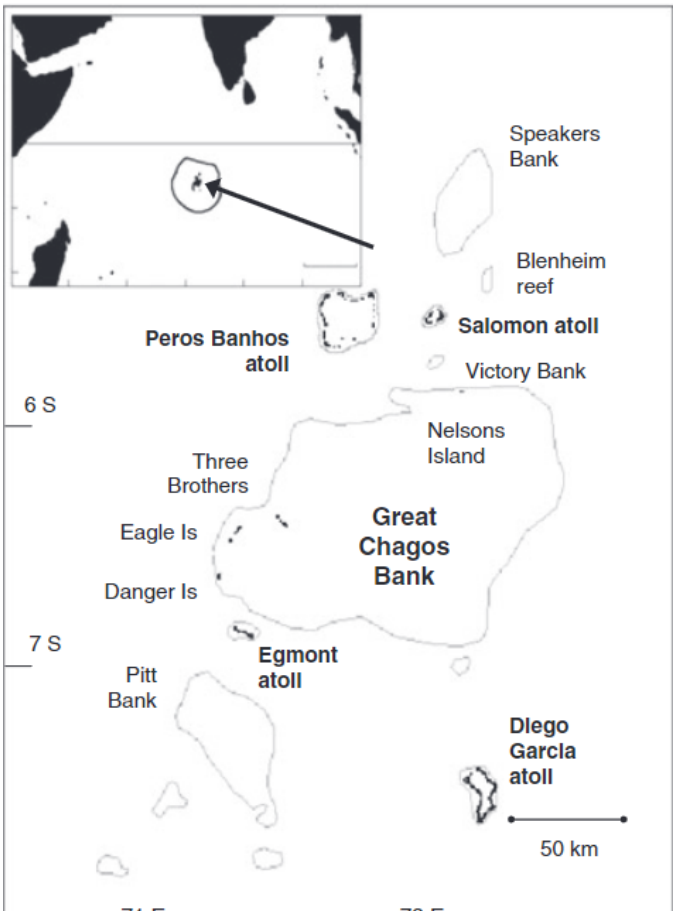

Figure 4: A map detailing the major islands and atolls of the Chagos Archipelago and (inset) it's location within the central Indian Ocean and (circled) the MPA boundary. Taken from Sheppard *et al.,* (2012).

1.4 Stable isotope analysis

Within the last few decades, stable isotope analysis (SIA) has emerged as an effective tool for the study of elasmobranch trophic ecology and habitat use, particularly that of threatened or elusive species (Shiffman *et al.*, 2012). SIA is based upon the principle that an organism's tissues will integrate isotopes from the organism's diet and environment and, thus, the tissues of the organism will reflect the organism's feeding ecology and habitat use (Peterson & Fry, 1987). The stable isotope ratios of carbon ($^{12}C/^{13}C$, $\delta^{13}C$) and nitrogen ($^{14}N/^{15}N$, $\delta^{15}N$) are used to investigate habitat use and trophic ecology, respectively (Peterson & Fry, 1987; Post, 2002). Values of $\delta^{15}N$ increase by approximately 3-4 ‰ per trophic level, a process called isotopic discrimination (Post, 2022). Therefore, the trophic position of a species can be determined by comparing the $\delta^{15}N$ value of its tissues with that of potential prey and predators (Post, 2002). Biogeochemical and oceanographic processes alter the $\delta^{13}C$ composition of primary producers and therefore $\delta^{13}C$ values reflect foraging location (Peterson & Fry, 1987; France, 1995, Silva *et al.,* 2019). In a marine coastal ecosystem, for example, benthic algae are enriched in $\delta^{13}C$ by approximately 5‰ compared to planktonic algae (France, 1995) and this principle has been applied to reveal novel findings in the feeding ecology of the oceanic manta ray (*Mobula birostris*) (Burgess *et al.,* 2016). Selecting a suitable tissue to use for stable isotope analysis requires careful consideration. Tissues differ in their isotopic turnover rate owing to the rate at which tissues turnover their proteins (Tieszen *et al.,* 1983). Elasmobranch muscle has an isotopic turnover rate greater than a year and thus reflects long-term foraging ecology (Munroe *et al.,* 2020). Fewer stable isotope studies use elasmobranch skin tissue. However, it is predicted that skin will have a higher isotopic turnover rate than muscle due to the faster protein turnover and therefore reveal short-term foraging behaviour over approximately several weeks (Carlisle *et al.,* 2012). Through stable isotope analysis of skin and muscle, it is possible to infer the feeding ecology and habitat use over both seasonal and annual scales (MacNeil *et al.,* 2005).

This study will use stable isotope analysis of *M. alfredi* muscle and skin tissue, with a focus on $\delta^{13}C$, to (i) investigate temporal variation in the feeding ecology and habitat use of *M. alfredi* and (ii) identify any distinct foraging habitats within the Chagos Archipelago. Overall, the research will enhance current

understanding of the local Chagos population of *M. alfredi* and provide direction for future research of *M. alfredi* within this region.

2. METHOD

2.1 Study area

Samples of *M. alfredi* and plankton were collected from various locations within the Chagos Archipelago in the central Indian Ocean (Figure 4). Geographically, Chagos is situated in the central Indian Ocean however, it is recognised by the IUCN as part of the Western Indian Ocean region (Fischer & Bianchi, 1984; Bullock *et al.,* 2021) due to the oceanographic and biological similarities between Chagos and the western Indian Ocean (Sheppard *et al.,* 2012; Carr *et al.,* 2022). Therefore, this paper will refer to Chagos in the context of the western Indian Ocean. Chagos lies on the eastern edge of the Seychelles-Chagos Thermocline Ridge (SCTR) and is subject to large-scale oceanographic changes caused by the Indian Ocean Dipole (IOD) (Dilmahamod *et al.,* 2016).

2.2 Sample collection

2.2.1 Mobula alfredi

Across three expeditions between 2019-2021, a total of 41 tissue biopsies were collected from individual *M.alfredi* from Egmont (n = 32), Salomon (n = 8) and Peros Banhos (n = 1) (Figure 5) from 24 females (adult = 5, juvenile = 19) and 17 males (adult = 11, juvenile = 6). The tissue biopsies were collected from individuals in November 2019 (n = 20), March 2020 (n = 6) and November 2021 (n = 15) (*see appendix A*). Samples were collected from the posterior dorsal surface of *M. alfredi* using a modified Hawaiian hand sling to deploy a biopsy dart. All biopsy activities were approved by the University of Plymouth Animals in Science Ethics Committee under permits ETHICS-24-2019 and ETHICS-37-2020. *Mobula alfredi* individuals were photographed from the ventral side for photo-ID of unique ventral markings. The size class, which acts as a proxy for maturity (Stevens, 2016), was visually estimated and sex of individuals was recorded. Biopsy samples were stored on ice and transported to the wet laboratory within 2 hours of collection. Of the 41 biopsy samples, 39 contained both white

muscle and skin which were later separated and 2 contained only skin (n = 1) or muscle (n = 1). Once separated, all muscle (n = 40) and skin (n = 40) samples were oven-dried at 60°C for 24 hours. The dried samples were transported to the University of Plymouth in a cool box for further processing.

2.2.2 Plankton collection

A total of 70 plankton samples were collected from the top 2 m of the water column from Egmont (n = 42), Salomon (n = 11), Peros Banhos (n = 9), Nelson Island (GCB) (n = 3) and Three Brothers (GCB) (n = 5) (Figure 5). Plankton samples were collected opportunistically across all three sampling years. Presence or absence of feeding *M. alfredi* in the area at the time of plankton collection was recorded. Plankton were collected using a plankton net of 100 µm mesh size, a 50 cm diameter mouth opening, a 1:4 mouth-length ratio and a 100 µm mesh bag style cod-end. The volume of water filtered during each tow was measured using a flowmeter attached in the centre of the mouth opening. Plankton samples were stored on ice and transported to the laboratory where they were split using a Folsom splitter. One half of the plankton samples were dried in an oven at 60°C for 24 hours before being transported to the University of Plymouth in a cool box.

2.3 Sample processing

2.3.1 Lipid extraction

All muscle, skin, and plankton samples were treated to remove lipids. Within a tissue, lipids are depleted in ^{13}C relative to carbohydrates and proteins (DeNiro & Epstein, 1977). A high lipid content within a tissue can result in bias of SIA results of $\delta^{13}C$ (Hussey *et al.*, 2012a). Removal of lipids for stable isotope analysis has been recommended for elasmobranch tissue (Hussey *et al.,* 2012b; Li *et al., 2*016) and for plankton (Marcus *et al*., 2017). Lipid removal was performed using a wash of chloroform-methanol at a 2:1 concentration as described by Folch *et al.,* (1957). Samples were soaked in a 2:1 chloroform-methanol solution in 7 mL glass vials for 24 hours and then air dried for 24 hours (Carlisle *et al.*, 2017; Peel *et al.*, 2019).

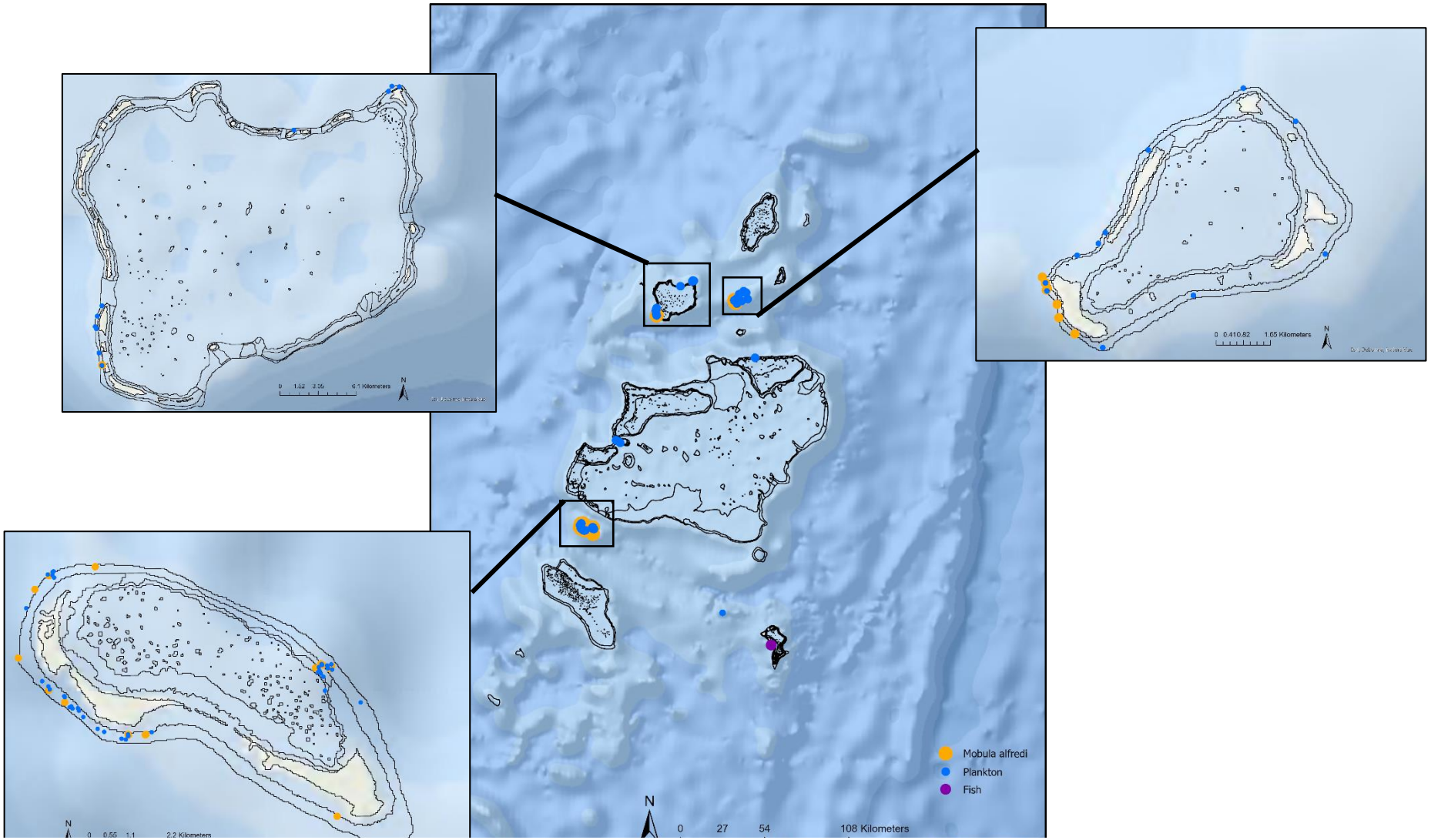

Figure 5: Sampling site locations in the Chagos Archipelago of *M. alfredi*, plankton, and fish. Egmont, Peros Banhos and Salomon are shown enlarged clockwise from bottom left.

2.3.2 Urea extraction

Elasmobranch tissues contain high levels of urea due to the retention of urea for osmoregulation (Hussey *et al.*, 2012b). Urea is depleted in ^{15}N and therefore causes bias in stable isotope results of $\delta^{15}N$ (Li *et al.*, 2016). Removal of urea for stable isotope analysis has been recommended for elasmobranch tissue (Kim & Koch, 2012; Li *et al.*, 2016). Muscle and skin samples were soaked in 1.5 mL of MilliQ water for 24 hours at room temperature. After 24 hours, samples were centrifuged at 3,000rpm for 3 minutes and the excess MilliQ water was removed. The urea extraction process was repeated a further two times, replacing with fresh MilliQ water each cycle. At the end of the third cycle, the samples were oven dried at 60°C for 48 hours. (Marcus *et al.*, 2017; Peel *et al.*, 2019).

2.4 Stable isotope analysis

Once dried, all *M. alfredi* and plankton samples were weighed using a microbalance. Plankton and muscle were weighed to 800 µg ± 10% and skin was weighed to 1000 µg ± 10%. Samples were placed in tin capsules and sent to the University of Exeter for mass spectrometry analysis.

Stable isotope signatures are calculated as ratios using the equation:

$$\left[\left(\frac{R_{sample}}{R_{standard}}\right) - 1\right] x\ 1000$$

where R = $^{13}C/^{12}C$ or $^{15}N/^{14}N$. R_{sample} refers to the isotopic ratio within the tissue sample and $R_{standard}$ refers to an internationally recognised standardised baseline isotopic ratio derived from Vienna PeeDee Belemite (VPDB) for $\delta^{13}C$ and atmospheric N_2 for $\delta^{15}N$ (Post, 2002). The stable isotope signature is denoted as the ratio of the heavier isotope to the lighter isotope, using δX where X = the heavier isotope e.g., $\delta^{13}C$, $\delta^{15}N$ (Peterson & Fry, 1987).

2.5 Statistical analyses

2.5.1 ANOVAs

One-way ANOVAs were used to investigate differences in the $\delta^{15}N$ and $\delta^{13}C$ values between *M. alfredi* muscle, skin, and bulk plankton samples across all years. For muscle and skin, the effect of sex, maturity,

sampling year and sampling location were assessed to identify any intra-specific variation in isotope signatures. Bulk plankton samples were divided by atoll and sampling year to investigate variation in plankton isotopic signatures. Prior to analysis, data was confirmed to be normally distributed and homogeneous using Shapiro-Wilk normality test and Levene's test, respectively. Where data assumed normality and was homogeneous, one-way ANOVA with Tukey's honesty *post hoc* test were used. Where data were non-normally distributed or heterogeneous, Welch's ANOVA with Games-Howell *post hoc* test were used. All analyses were conducted in R (version 4.1.2; R Core Team 2021) and significance was set at $p < 0.05$. Variation around the mean is expressed as standard deviation unless stated otherwise.

2.5.2 Bayesian analysis

Bayesian Stable Isotope Mixing Models were created in R using the package *simmr* (Parnell, 2016) to assess the probable contribution of plankton from different locations throughout the Chagos Archipelago to the diet of *M. alfredi*. Plankton sources were grouped by atoll and divided into more precise locations when sample size was sufficient, giving a total of eight potential sources. $\delta^{13}C$ and $\delta^{15}N$ values from further five plankton samples collected from Sandes Seamount in 2022 (Harris and Eager, unpublished data) were incorporated into the data (*see appendix B*). Diego Garcia is a location where *M. alfredi* are frequently sighted, however no plankton or *M. alfredi* samples were collected from this location. Instead, 31 muscle samples of rainbow runner *(Elagatis bipinnulata)*, bluefin trevally *(*Caranx melampygus*)* and bohar snapper *(Lutjanus bohar*) provided $\delta^{13}C$ and $\delta^{15}N$ values (Curnick, unpublished data) to act as a proxy for plankton in this location (*see appendix B*). For fish samples, estimated $\delta^{13}C$ and $\delta^{15}N$ values were adjusted based on the trophic enrichment factor (TEF, Δ) calculated using the mean $\delta^{13}C$ and $\delta^{15}N$ values of *M. alfredi* and fish samples using the equation

$$\Delta X = \delta X_{consumer} - \delta X_{prey,}$$

where X represents $\delta^{13}C$ or $\delta^{15}N$ (Fry, 2006). This resulted in TEFs of 2.3 ± 0.48 for $\delta^{13}C$ and -2.5 ± 2.7 for $\delta^{15}N$. For plankton samples, TEFs were calculated using the same equation from plankton sampled only when mantas were observed feeding (n = 36) (Couturier *et al.,* 2013). The final model included a total of

eight locations: Salomon Atoll, Peros Banhos Atoll, Egmont Lagoon, Egmont outer atoll (hereafter Egmont Outside), Nelson Island (north Great Chagos Bank), Three Brothers (west Great Chagos Bank), Sandes Seamount and Diego Garcia Atoll. Concentration dependents were included into the *simmr* analysis to account for the varying percentages of carbon and nitrogen in the bulk plankton and fish samples which would otherwise give biased proportional input. The percentages of C and N are calculated through mass spectrometry and are included in the overall stable isotope results. The mean concentration dependent of plankton samples are calculated for the same atolls and locations used for the TEFs.

3. RESULTS

3.1 Inter-tissue variation

Plankton are depleted in $\delta^{13}C$ and $\delta^{15}N$ compared to both muscle and skin of *M. alfredi*. Skin and muscle display similar mean $\delta^{13}C$ and $\delta^{15}N$ values (Table 1). Muscle has a lower mean $\delta^{13}C$ and higher mean $\delta^{15}N$ value than skin (Table 1, Figure 6). Welch ANOVA with Games-Howell *post hoc* test show a significant enrichment of *M. alfredi* muscle and skin in $\delta^{15}N$ compared to plankton (Welch ANOVA $F_{2,386} = 96.031$, $p<0.001$) with Games-Howell *post hoc* test showing significant enrichment between muscle and plankton ($p<0.001$); skin and plankton ($p<0.001$) and muscle and skin ($p<0.001$) (*see Appendix C)*. *Mobula alfredi* muscle and skin are significantly enriched in $\delta^{13}C$ compared to plankton (Welch ANOVA $F_{2,51} = 84.022$, $p<0.001$). Games-Howell *post hoc* test shows significant enrichment of $\delta^{13}C$ between muscle and plankton ($p<0.001$), skin and plankton ($p<0.001$) and muscle and skin ($p=0.001$) (*see Appendix C)*.

Table 1: The sample size, minimum, maximum, range, and mean (± SD) of $\delta^{13}C$ and $\delta^{15}N$ of *M. alfredi* muscle, skin, and bulk plankton.

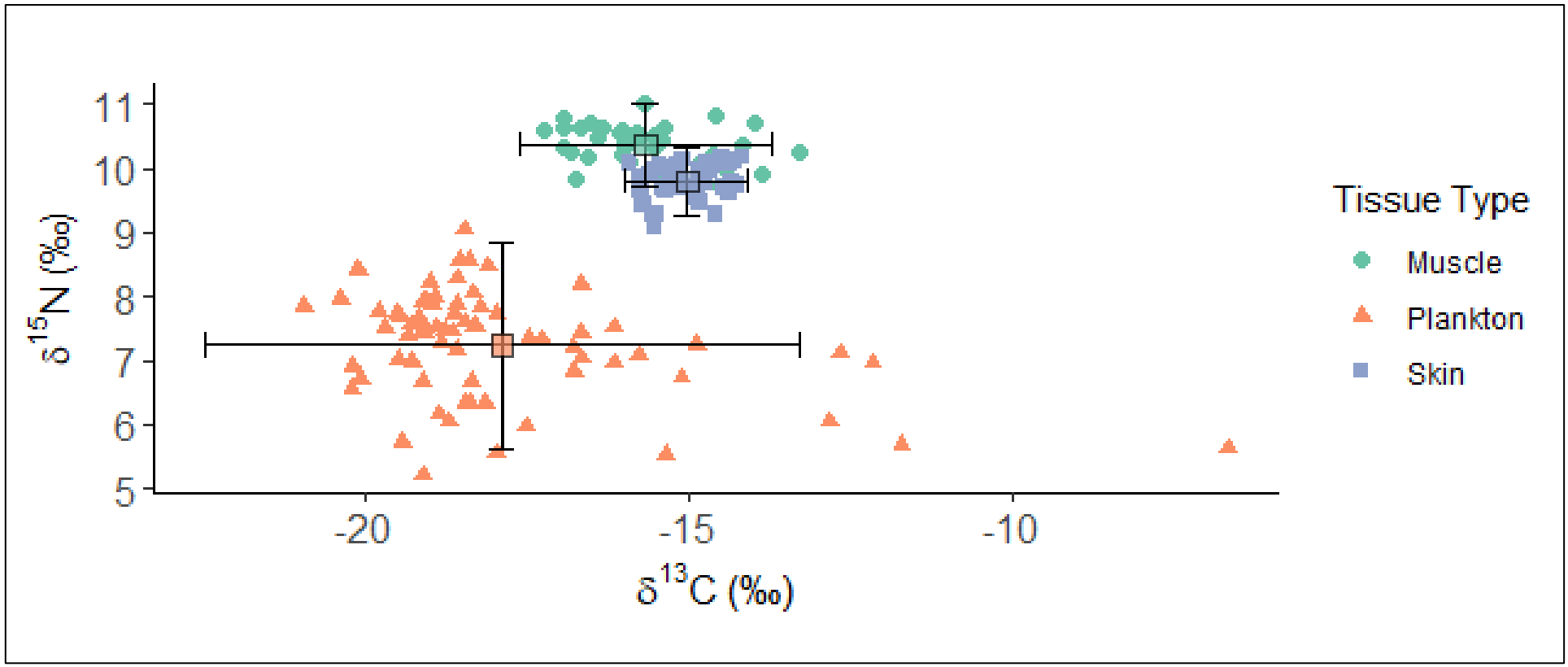

Figure 6: Isotopic biplot of the individual isotopic signatures of *M. alfredi* muscle, *M. alfredi* skin, and plankton. Error bars indicate 95% confidence intervals. Black square represents the mean.

3.2 Annual variation

Between years, the $\delta^{15}N$ values of *M. alfredi* muscle and skin did not differ (ANOVA, $F_{2,37} = 1.499$, $p = 0.237$; ANOVA, $F_{2,37} = 0.8424$, $p = 0.403$, respectively). $\delta^{13}C$ values of *M. alfredi* muscle did not differ between year (ANOVA, $F_{2,37} = 0.9$, $p = 0.415$). $\delta^{13}C$ values of *M. alfredi* skin showed a difference between years (ANOVA, $F_{2,37} = 6.4$, $p = 0.0041$). Tukey's post-hoc comparison test indicated a significant difference in $\delta^{13}C$ values of skin between 2019-2020 (THSD, $p = 0.014$, 95% C.I = [1.082, 0.104]) and 2019-2021 (THSD, $p = 0.018$, 95% C.I. = [0.783, 0.062]) (Figure 7). Bulk plankton $\delta^{13}C$ values did not differ between years (ANOVA $F_{2,66} = 0.223$, $p = 0.801$). However, plankton $\delta^{15}N$ did show annual differences (Welch ANOVA $F_{2,47} = 27.989$, $p<0.001$) and plankton samples were significantly enriched in $\delta^{15}N$ in 2019 compared to 2020 (Games-Howell $p<0.001$) and enriched in 2021 compared to 2020 (Games-Howell $p<0.001$).

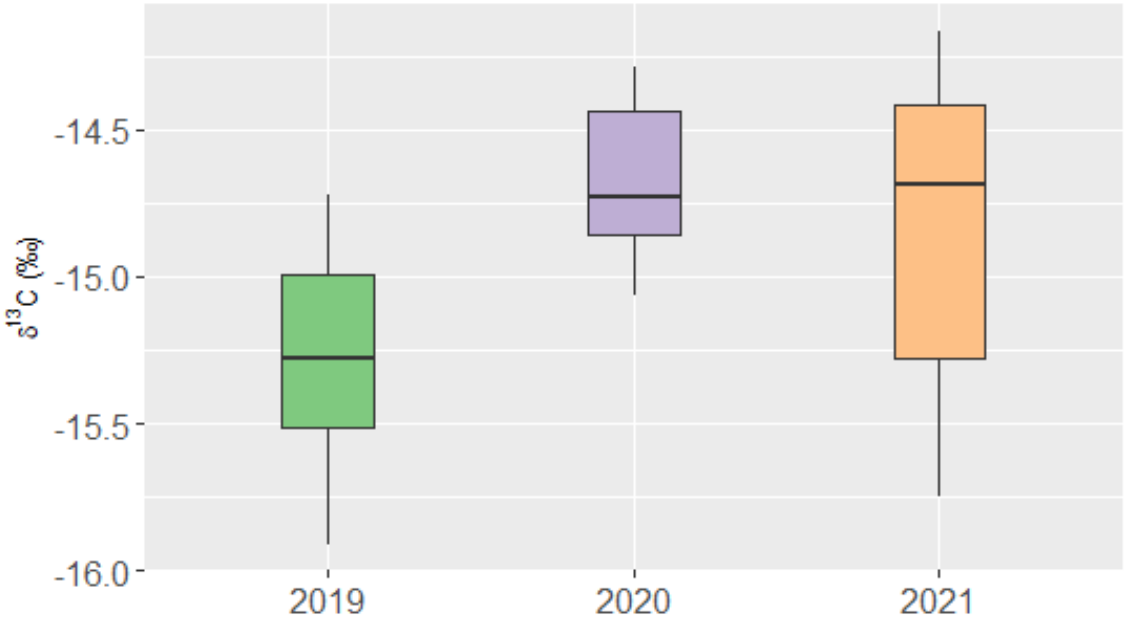

Figure 7: Boxplot of *M. alfredi* skin $\delta^{13}C$ values from 2019, 2020 and 2021. Coloured boxes encompass the interquartile range, the middle line denotes the median and the whiskers show the minimum and maximum values.

3.3 *Spatial variation*

To test for spatial variation in isotopic signatures, *M. alfredi* were grouped into 'northern' (Peros Banhos and Salomon) and 'southern' (Egmont), which are approximately 150 km apart. $\delta^{15}N$ values of *M. alfredi* muscle and skin did not differ with respect to sampling location (ANOVA, $F_{1,38} = 2.727$, $p = 0.107$; ANOVA, $F_{1,38} = 2.159$, $p = 0.15$, respectively). $\delta^{13}C$ values of *M. alfredi* muscle did not differ between northern and southern atolls (ANOVA, $F_{1,38} = 0.014$, $p = 0.908$) however $\delta^{13}C$ values of skin from *M. alfredi* sampled in the south were depleted compared to those from northern atolls (ANOVA $F_{1,38} = 9.771$, $p = 0.003$) (*see Appendix D)*. As there was a significant difference between years, *M. alfredi* were further divided by location and year. 2021 was the only year in which *M. alfredi* were sampled from both northern and southern atolls. In 2021, *M. alfredi* skin showed depleted $\delta^{13}C$ values from southern atolls compared to northern atolls (One-way ANOVA $F_{1,13}=5.31$, $p = 0.038$) (Figure 8).

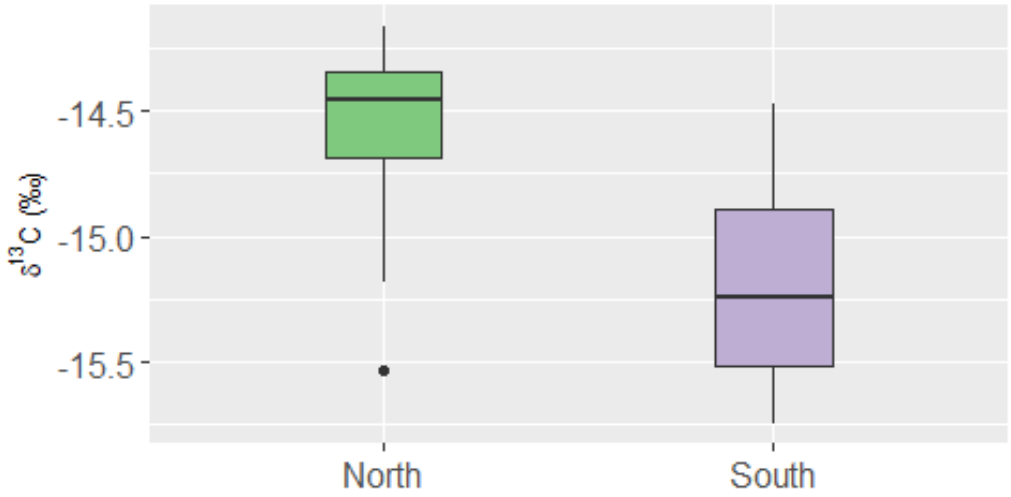

Figure 8: Boxplot of $\delta^{13}C$ values of *M. alfredi* skin from *M. alfredi* sampled in the north (Peros Banhos and Salomon) and the south (Egmont) in 2021 only. Coloured boxes encompass the interquartile range, the middle line denotes the median and the whiskers show the minimum and maximum values. Outliers are represented by circles.

When grouped by the locations: Salomon, Peros Banhos, Great Chagos Bank, and Egmont, plankton $\delta^{13}C$ values did not vary with location (ANOVA, $F_{2,39} = 1.041$, $p = 0.363$*).* $\delta^{15}N$ values showed a difference

between atolls (ANOVA, $F_{3,65} = 3.158$, p=0.031), however no significant pair-wise differences were observed following Tukey's Honesty post hoc test.

3.4. Bayesian stable isotope mixing models

Bayesian *simmr* analyses were performed to estimate the proportional contribution of planktonic prey from different locations into the diets of *M. alfredi*. Due to the inter-annual difference of skin $\delta^{13}C$ values, three separate mixing models were constructed, one for each year. A mixing model was created for *M. alfredi* grouped by location and year (i.e. 2021 north and 2021 south). As there were no apparent inter-annual or intra-specific differences in isotope values for muscle, one mixing model was created to incorporate all muscle data.

Mixing model results estimated the proportion of input of plankton from each location to the diet of *M. alfredi* in 2019, 2020 and 2021 (Figure 9). The isotopic signatures of *M. alfredi* skin in 2019, 2020 and 2021 and bulk plankton from eight locations reveal clear overlap of *M. alfredi* with all of the source locations aside from Sandes (Figure 9a). Bayesian analysis suggest that in 2019 the largest contributor to diet is plankton from Peros Banhos (approx. 23%) followed by Egmont Lagoon (approx. 20%). In 2020, the mixing model results are much more homogenous, perhaps due to the smaller sample size of *M. alfredi* in 2020, yet plankton from Egmont Lagoon and Nelson appear to be the largest contributors to diet (approx. 14%). Plankton from Egmont lagoon form approximately 25% of *M. alfredi* diet in 2021 and are the largest contributor to diet in 2021. Unlike 2019, plankton from Peros Banhos contribute less to *M. alfredi* diet in 2021 (approx. 14%). Consistently across all years, plankton from Sandes Seamount contributes relatively little compared to other locations. (Figure 9 b-d).

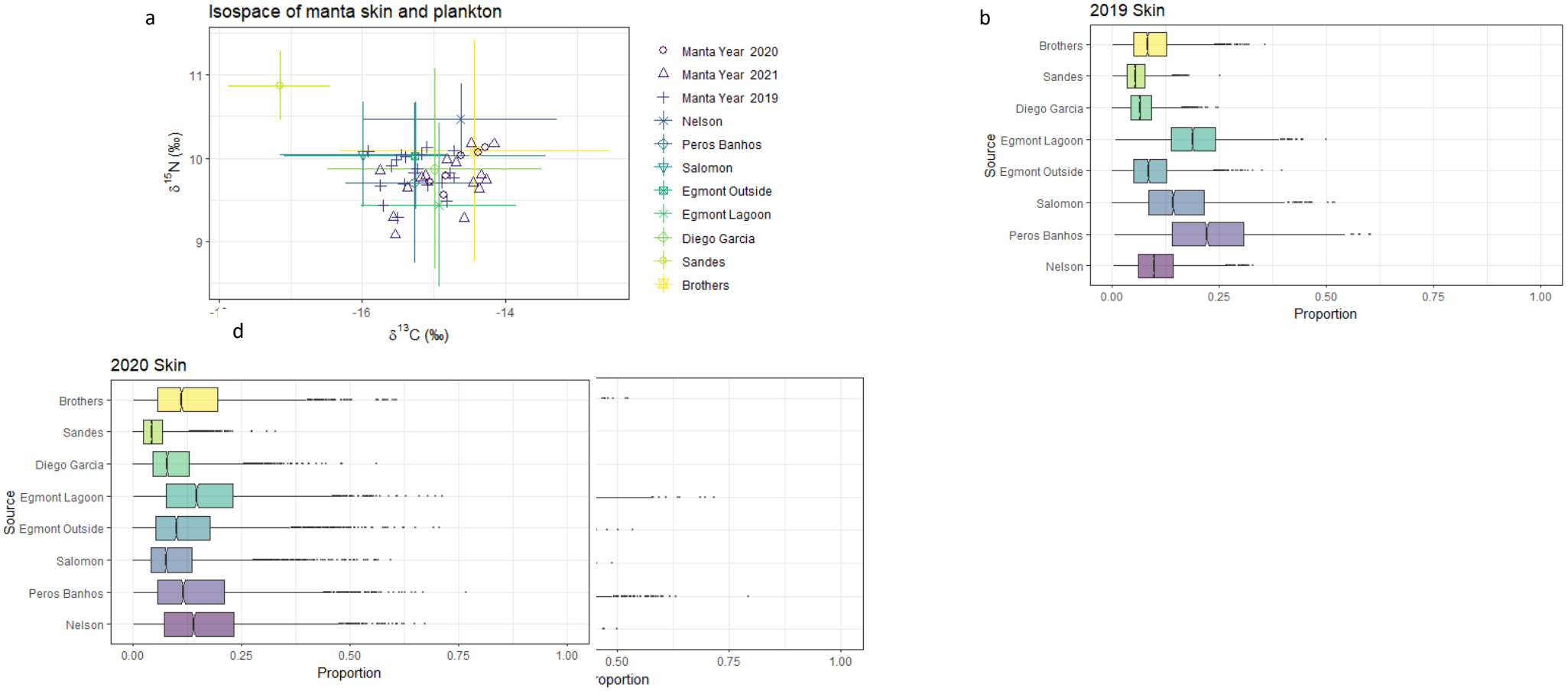

Figure 9: (a) Isotopic biplot of *M. alfredi* skin isotope signatures from 2019, 2020 and 2021 in relation to isotopic signatures of plankton from different locations within the Chagos MPA. Proportional contribution of plankton from different locations to the diets of *M. alfredi* in (b) 2019, (c) 2020 and (d) 2021 estimated using Bayesian mixing models. Boxplots show the interquartile range (coloured box), median and maximum and minimum values (whiskers) of source contribution to *M. alfredi* diet.

Bayesian analysis estimates the proportion of diet input for *M. alfredi* sampled in the north and in the south in 2021 (Figure 10). The isotopic biplot shows considerable overlap of *M. alfredi* with all source locations except Sandes (Figure 10a). Estimates from the analysis predicts Egmont Lagoon as the primary contributor to northern *M. alfredi* diet in 2021 (approx. 25%) whereas southern *M. alfredi* in 2021 have similar dietary intake from Egmont Lagoon and Peros Banhos (approx. 15%) (Figure 10 b-c). Northern *M. alfredi* in 2021 display considerably more variation in foraging location than their southern counterparts (Figure 10 b-c). Sandes Seamount contributes relatively little to the diets in both the northern and southern *M. alfredi* (<5% for north and approx. 6% for the south).

The isotopic signatures of plankton and *M. alfredi* muscle overlap across all locations with the exception of Sandes Seamount (Figure 11a). The Bayesian mixing model results estimate that the highest dietary input revealed from *M. alfredi* muscle comes from Peros Banhos (approx. 23%) followed by Egmont Lagoon (approx. 20%). Brothers and Nelson (Great Chagos Bank), Egmont Outside and Salomon all have similar proportional input (approx. 10-15%). Sandes seamount and Diego Garcia show the smallest probable contribution to diet (<5%) (Figure 11b).

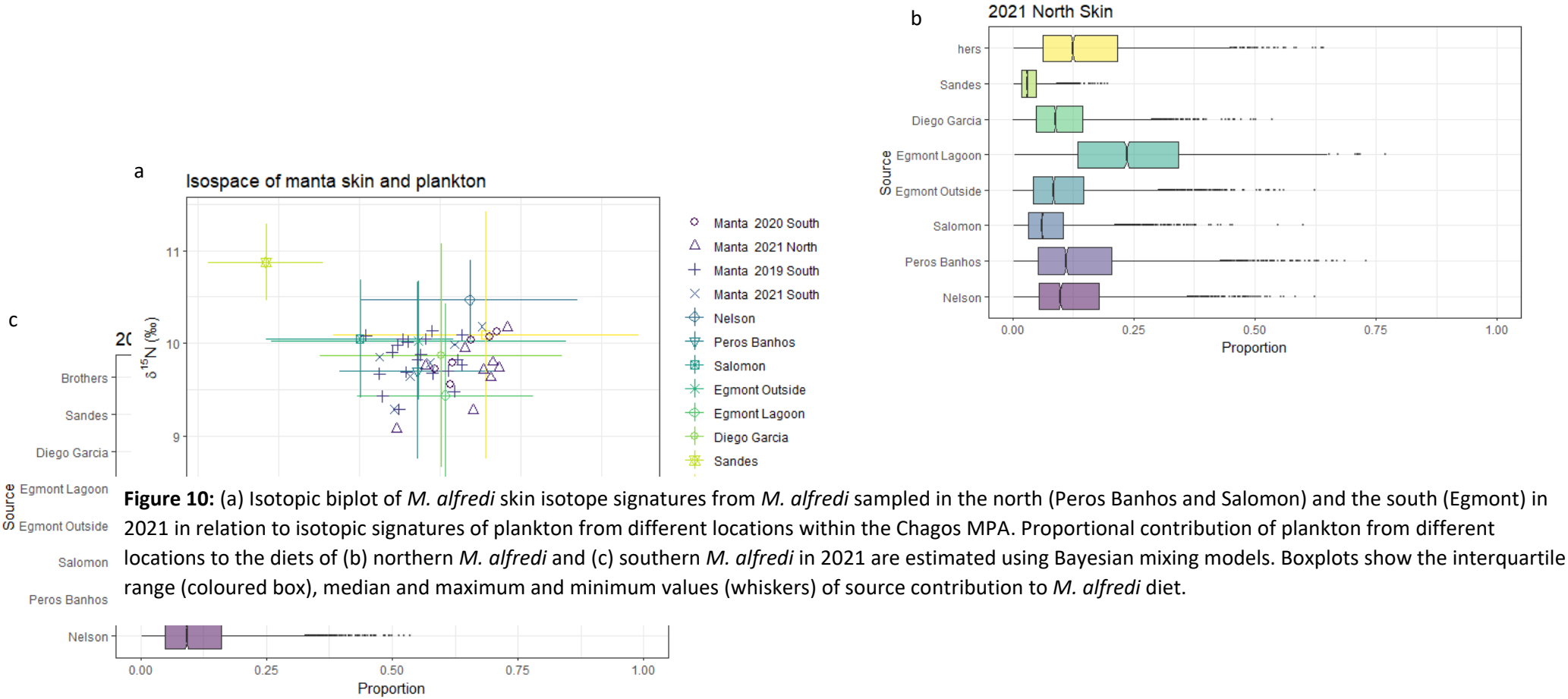

Figure 10: (a) Isotopic biplot of *M. alfredi* skin isotope signatures from *M. alfredi* sampled in the north (Peros Banhos and Salomon) and the south (Egmont) in 2021 in relation to isotopic signatures of plankton from different locations within the Chagos MPA. Proportional contribution of plankton from different locations to the diets of (b) northern *M. alfredi* and (c) southern *M. alfredi* in 2021 are estimated using Bayesian mixing models. Boxplots show the interquartile range (coloured box), median and maximum and minimum values (whiskers) of source contribution to *M. alfredi* diet.

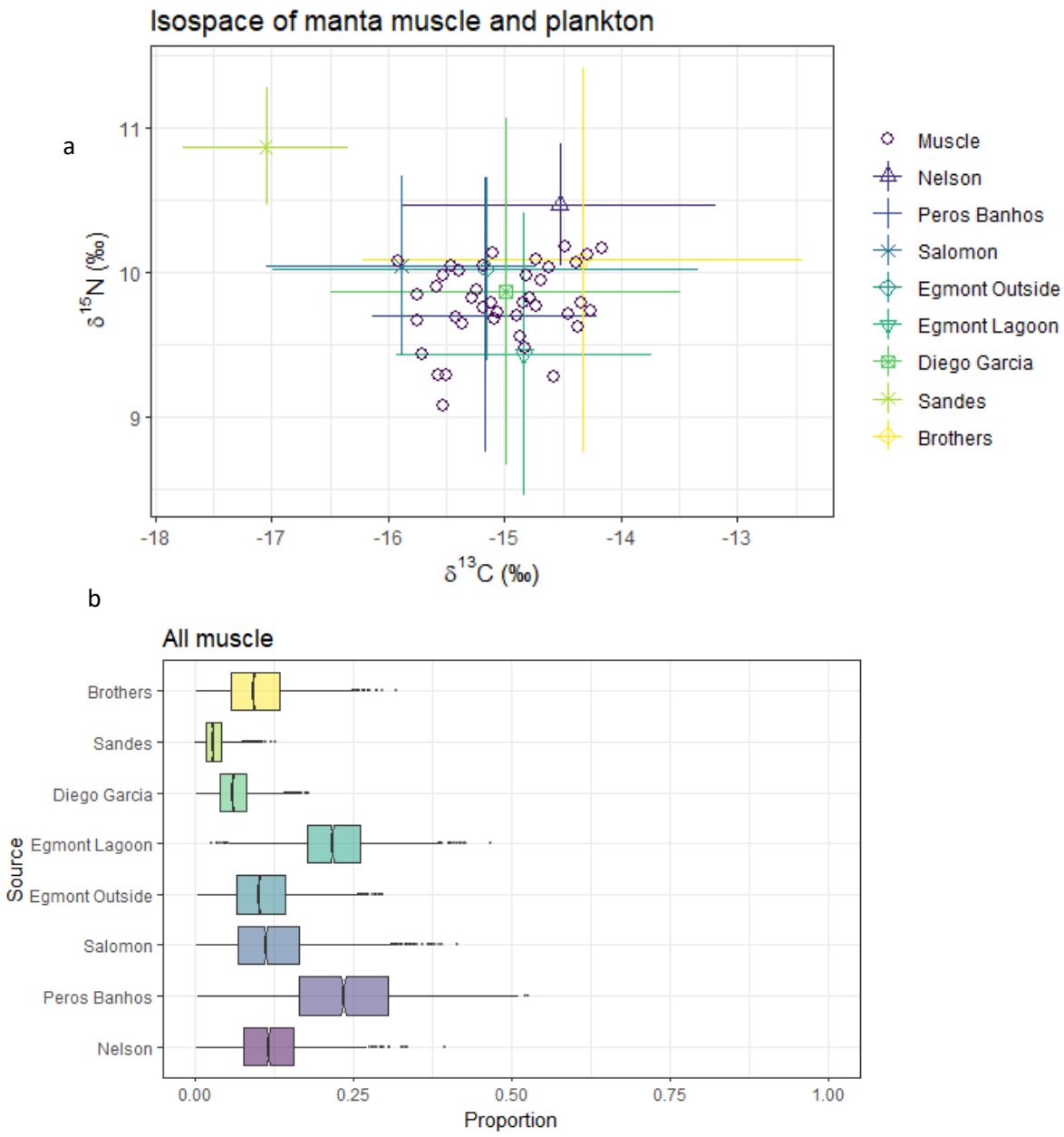

Figure 11: (a) Isotopic biplot of all *M. alfredi* muscle isotopic signatures in relation to plankton isotopic signatures grouped by locations within the Chagos MPA. Proportional contribution of plankton from different locations to the diets of *M. alfredi* estimated using Bayesian mixing models. Boxplots show the interquartile range (coloured box), median and maximum and minimum values (whiskers) of source contribution to *M. alfredi* diet.

4. DISCUSSION

This study uses stable isotope analysis to provide an insight into the feeding ecology and habitat use of *M. alfredi* in the Chagos Archipelago. Bayesian mixing models across all analyses suggest that *M. alfredi* feed predominantly at Egmont Lagoon and Peros Banhos (approx. 20-25% of diet input). These findings are consistent for both skin and muscle tissue, indicating that *M. alfredi* had been feeding at these locations several weeks and over a year prior to sampling.

4.1 Spatial variation

Results from the Bayesian mixing model for muscle tissue reveal clear disparity in habitat use with Egmont Lagoon and Peros Banhos as highly probable foraging locations (approx. 20-25% diet input) and Sandes Seamount and Diego Garcia as minimal contributors to diet (<5% diet input). A similar result is shown for *M. alfredi* skin tissue across all years. Egmont Atoll is a known feeding 'hotspot' for *M. alfredi* (Harris *et al*., 2019; 2021) and a total of 430 sightings with confirmed photo identification of *M. alfredi* individuals have been reported since 2013 at Egmont following surveys conducted by The Manta Trust (Harris, unpublished data). The preference for Egmont as a foraging location is thought to be due to the oceanographic conditions and shallow bathymetry which allow for increased upwelling of nutrients and consequent large zooplankton blooms (Harris *et al.,* 2021). The consistency across skin and muscle suggests that *M. alfredi* had been substantially feeding at Egmont Lagoon within the several weeks prior to sampling and previous year. Overall, the stable isotope analysis supports previous knowledge of *M. alfredi* foraging at Egmont.

Similarly, the mixing model results of muscle isotopic signatures place Peros Banhos as an equal contributor to *M. alfredi* diet as Egmont Lagoon (approximately 23%). In fact, mixing model results of skin in 2019 indicate that plankton from Peros Banhos formed a slightly larger contribution to the diet of *M. alfredi* than plankton from Egmont Lagoon. Peros Banhos has, however, received relatively little survey effort in comparison to Egmont and a total of 5 sightings with confirmed photo identification of *M. alfredi* have been reported between 2005-2021 (Harris unpublished data). To date, there is minimal

evidence of *M. alfredi* using Peros Banhos on a regular basis and the high proportion of diet input from Peros Banhos gives good reason to increase survey effort in this area of the Chagos Archipelago with the potential of confirming an *M. alfredi* foraging hotspot. Incentive to increase survey efforts at Peros Banhos is exacerbated by the high threat of illegal catch of *M. alfredi* at foraging hotspots.

Although the Chagos MPA is covered by a blanket no-take policy, IUU fishing poses a significant threat to species within the Chagos MPA and has been shown to have caused declines in shark species (Hays *et al.,* 2020). Acoustic telemetry and visual observations confirm the illegal fishing of an estimated >1000 grey reef shark (*Carcharhinus amblyrhynchos*) and silvertip shark (*Carcharhinus albimarginatus*) in December 2014 alone (Tickler *et al.,* 2019). It is, therefore, reasonable to predict that the threat of IUU fishing extends to *M. alfredi* and, in foraging hotspots where *M. alfredi* presence is greater, the threat will be heightened. A single enforcement vessel detects IUU fishing activity, however the large area of the Chagos MPA poses a huge challenge to enforcement and, since the designation of the MPA in 2010, the number of IUU vessel encounters has not decreased (Hays *et al.,* 2020). IUU activity is suspected to be concentrated in the northern regions of the MPA and illegal fishing vessels have been intercepted at Egmont and Peros Banhos (Ferretti *et al.,* 2018; Hays *et al.,* 2020) confirming the need for further patrol efforts in these locations. A study by Jacoby *et al.* (2020) to track the spatial overlap of the grey reef shark (*Carcharhinus amblyrhynchos)* and silvertip shark (*Carcharhinus albimarginatus)* with illegal fishing vessels highlights western Peros Banhos as a potentially important area for enforcement patrol efforts. Increased survey efforts at Peros Banhos will afford clarity on the spatial dynamics of *M. alfredi* and should be combined with patrol vessel data to assess overlap with illegal fisheries.

The reasons why Peros Banhos may act as a foraging hotspot are varied and may be attributed to adjacent terrestrial biodiversity. The northern and eastern islands of Peros Banhos are home to the majority of Chagos' 18 species of breeding seabirds (Carr, 2015; Wu *et al.,* 2021). High seabird abundance is associated with increased nutrient leaching into marine ecosystems from nitrate-rich guano (McCauley *et al.,* 2021) which drives marine primary productivity and thus, zooplankton aggregation (Shatova *et al.,* 2016). In the Palmyra Atoll, central Pacific, movement patterns of the closely

related oceanic manta ray (*Mobula birostris)* are influenced by the abundance of seabirds on adjacent islands (McCauley *et al.,* 2021). Seabird abundance in Chagos is influenced by the presence of the invasive black rat (*Rattus rattus)* on at least 30 islands*,* which decimates seabird populations by predation on eggs and chicks (Jones *et al.,* 2008; Graham *et al.,* 2018, Harper *et al.,* 2019). The presence of rats on islands in Chagos has been shown to reduce nutrient leaching into the marine ecosystem by a factor of 251 (Graham *et al.,* 2018). Further research could incorporate terrestrial biodiversity data with fine-scale analysis of *M. alfredi* foraging locations, such as between the rat-free and rat-infested islands of Peros Banhos, which would enhance our understanding of terrestrial-marine ecological interactions in the MPA.

Contrarily, Bayesian mixing models place Diego Garcia in the southeast of the archipelago as a relatively low contributor to *M. alfredi* diet. The low probability of Diego Garcia as a feeding location is supported by the few photo identification samples of *M. alfredi* individuals in Diego Garcia (n=9) since 2005 (Harris, unpublished data). Satellite tracking data show two individual *M. alfredi* making a journey in excess of 130 km from Egmont to Diego Garcia (Harris, 2019). *Mobula alfredi* display high levels of site fidelity (Setyawan *et al.,* 2018) and it could be that *M. alfredi* make transient visits to Diego Garcia to feed away from their home site, hence the low diet input reflected from long-term muscle tissue. Another possibility is that Diego Garcia isn't a foraging location but instead a site of a cleaning station. Cleaning stations are an important part of *M. alfredi* ecology; they serve to rid individuals of parasites, algal growth, and bacteria and promote wound healing (Stevens *et al.,* 2018). To better understand how *M. alfredi* use the waters around Diego Garcia, it will be beneficial to include sampling and behavioural observations of *M. alfredi* in Diego Garcia into future research, especially as Diego Garcia is the only inhabited island and therefore may have anthropogenic effects on the coastal ecosystem.

Whilst *M. alfredi* display high site fidelity (Setyawan *et al.,* 2018), they are highly mobile elasmobranchs and are capable of swimming distances in excess of 1,000 km (Stevens *et al.,* 2018). Bayesian analysis of their skin isotopic signatures from *M.alfredi* sampled in the north of the archipelago compared to those sampled in the south of the archipelago in 2021 reveal that *M. alfredi* in the north are likely to feed at

Egmont Lagoon, some 150 km away. As skin reveals the isotopic consumption of several weeks prior, it is possible that *M. alfredi* were feeding at Egmont Lagoon and then travelled to Peros Banhos or Salomon, where they were sampled a few weeks later. Nonetheless, this suggests a corridor between Egmont and the north of the archipelago which, again, has potential to be exploited by IUU fishing. This is supported by previous satellite tracking data of *M. alfredi* by Harris (2019) that shows one *M. alfredi* individual making the journey between Egmont and Salomon, through the west of Great Chagos Bank. It is, therefore, important to not only identify areas of foraging but also identify the corridors between foraging habitats and other critical habitats such as cleaning stations.

4.2 Annual variation in habitat use

Annual variation between skin $\delta^{13}C$ values and between Bayesian mixing model estimates of foraging location could be attributed to large-scale, annual variability in oceanographic conditions, such as those caused by the Indian Ocean Dipole (IOD) (Saji *et al,* 1999; Huang *et al.,* 2022). The IOD is an ocean-atmosphere interaction that causes annual variability in sea surface temperatures and anomalous wind and precipitation events (Saji *et al.,* 1999). The IOD is associated with 'positive', 'negative' and 'neutral' cycles. A positive IOD cycle constitutes a warmer western Indian Ocean and cooler eastern Indian Ocean (Australian Government Bureau of Meteorology, 2012). Positive IOD phases are associated with a deepening of the thermocline in the western Indian Ocean which causes a change in the surface and subsurface phytoplankton concentration (Dilmahamod *et al.,* 2016). Thermoclines are associated with higher concentrations of chlorophyll-α, a signifier of high phytoplankton concentration, thus a deepening of the thermocline may result in lower surface plankton concentrations (Sharples *et al.,* 2001; Harris *et al.,* 2021). Moreover, the Seychelles-Chagos Thermocline Ridge (SCTR), on which Chagos lies on the eastern edge, is a prominent site of upwelling (Lee *et al.,* 2022). Upwelling is a process by which cold, nutrient-rich water from the deep rises to the surface, bringing with it high concentrations of plankton (NOAA). Upwelling events on the SCTR display interannual variability and are known to be supressed during positive IOD phases, therefore reducing the transport of nutrient-rich water from the deep to the surface (Lee *et al.,* 2022). High planktonic productivity is essential to support the energetic

demands of planktonic elasmobranch megafauna such as *M. alfredi* (Meekan *et al.,* 2015; Armstrong *et al.,* 2016). Variations in plankton availability influence the movement patterns of the largest of filter feeders, the whale shark (*Rhincodon typus*) in western Australia (Marcus *et al.,* 2019), *M. alfredi* in eastern Australia (Armstrong *et al.,* 2016) and pygmy blue whale (*Balaenoptera musculs brevicauda*) in Chagos (Huang *et al.,* 2022). Therefore, in Chagos, annual fluctuations of marine primary productivity are likely to drive *M. alfredi* to forage in variable locations.

In the boreal autumn of 2019, the Indian Ocean experienced the strongest positive IOD event of the 21st Century (Shi & Wang, 2021). In September and October of 2019, the suppression of upwelling and increased downwelling (the movement of warm surface water to deeper water), caused the deepening of the thermocline and sustained depletion of nutrients for phytoplankton growth (Shi & Wang, 2021). During this positive IOD phase, chlorophyll-α concentration in the western Indian Ocean was significantly reduced by over 30% compared to that of normal years and remained at low levels until May 2020 (Shi & Wang, 2021). The decreased phytoplankton concentration will have subsequently lowered the availability of zooplankton prey for *M. alfredi*. Skin isotopic signatures of *M. alfredi* reflect the feeding events of the several weeks prior to sampling. In the case of *M. alfredi* sampled in November 2019, this would coincide with the start of the peak of the extreme positive IOD event. Fluctuations in zooplankton abundance will drive *M. alfredi* to seek productive foraging grounds, which could be in deeper waters or further offshore, potentially out of the MPA boundary and into unprotected waters. Future research to link large-scale, annual changes in oceanographic conditions with patterns of *M. alfredi* movement and feeding ecology should be conducted. This is especially relevant as climate change is predicted to increase the frequency of extreme positive IOD events three-fold to once every six years (Cai *et al.,* 2014). With success, movement patterns of *M. alfredi* could be predicted with the IOD which can be predicted a few months prior to occurrence (Zhao *et al.,* 2019).

4.3 Inter-tissue variation

Upon reviewing the literature, it is evident that many stable isotope studies of elasmobranch species utilise muscle tissue to identify long-term foraging patterns (e.g. Daly *et al.,* 2013; Shiffman *et al.,* 2014;

Burgess *et al.,* 2016; Peel *et al.,* 2019), but few analyse skin tissue to reveal short-term feeding ecology and habitat use (e.g. Marcus *et al.,* 2019). Tissues which display similarly short turnover times are often used instead, for example liver or plasma (Shiffman *et al.,* 2012), the former of which requires lethal sampling (MacNeil *et al.,* 2005; Shiffman *et al.,* 2012) and the latter uses an alternative sampling method and equipment to muscle (Kim & Koch, 2012). Skin, on the other hand, can be sampled using the same biopsy technique as muscle with a minimally invasive procedure to collect one sample which can be separated, as demonstrated in this study. The results from this study reveal a significant difference in the isotopic signatures of $\delta^{13}C$ between *M. alfredi* muscle and skin tissue, demonstrating that skin reveals patterns in feeding ecology unique to those from muscle. Additionally, stable isotope analysis identifies a significant depletion in the $\delta^{13}C$ signatures of *M. alfedi* skin sampled in the south (Egmont) compared to those from the north (Salomon and Peros Banhos). Muscle tissue, however, does not show any significant difference in $\delta^{13}C$ values between northern and southern mantas. The disparity in results shown by skin and muscle is further evidence of why skin should be used in conjunction with muscle in stable isotope studies as it has the potential to reveal finer-scale aspects of feeding ecology that muscle overlooks. Therefore, future stable isotope studies should consider using skin to investigate seasonal (short-term) variations in feeding ecology and habitat use. Knowledge of seasonal habitat use is critical for the application of dynamic management practices (Arcangeli *et al.,* 2017; Harris *et al.,* 2020). For example, the IUU fishing patrol vessel bases its patrols on arrest history and radio intelligence or to cover discrete geographical features such as seamounts (Jacoby *et al.,* 2020). Our results suggest that Sandes Seamount contributes very little to *M. alfredi* feeding. Therefore, focusing patrol efforts over seamounts without empirical data to support seamounts as key habitat for *M. alfredi* does little to support effective *M. alfredi* protection. Secondly, this is a relatively static approach to a patrol and instead, a thorough understanding of species' movement patterns on a seasonal basis would allow the patrol vessel to target high-risk areas at appropriate times of the year.

5 CONCLUSION

Overall, this research has provided an insight into the feeding ecology and habitat use of *M. alfredi* within the Chagos MPA and given direction for future research. It has provided evidence that *M. alfredi* in the Chagos MPA may be feeding at Peros Banhos in the north of the archipelago, an atoll where survey efforts of *M. alfredi* have been relatively low and is potentially a site of high overlap with illegal fisheries. Temporal variations in foraging location highlight the need for dynamic management practices with respect to enforcing the MPA's no-take policy and to best protect *M. alfredi* from continued exploitation at the hands of illegal fisheries. Stable isotope analysis has allowed us to advance our understanding of *M. alfredi* feeding ecology and habitat use which is vital to support their conservation and maintain the Chagos MPA as a refuge in the highly exploited Indian Ocean.

REFERENCES

Agyeman, N. A., Blanco-Fernandez, C., Steinhaussen, S. L., Garcia-Vazquez, E., & Machado-Schiaffino, G. (2021). Illegal, unreported, and unregulated fisheries threatening shark conservation in African waters revealed from high levels of shark mislabelling in Ghana. *Genes*, *12*(7): 1002, https://doi.org/10.3390/genes12071002

Andrzejaczek, S., Chapple, T. K., Curnick, D. J., Carlisle, A. B., Castleton, M., Jacoby, D. M. P., Peel, L. R., Schallert, R. J., Tickler, D. M., & Block, B. A. (2020). Individual variation in residency and regional movements of reef manta rays *Mobula alfredi* in a large marine protected area. *Marine Ecology Progress Series*, *639*, 137–153. https://doi.org/10.3354/meps13270

Arcangeli, A., Campana, I., & Bologna, M. A. (2017). Influence of seasonality on cetacean diversity, abundance, distribution and habitat use in the western Mediterranean Sea: Implications for conservation. *Aquatic Conservation: Marine and Freshwater Ecosystems*, *27*(5), 995–1010. https://doi.org/10.1002/aqc.2758

Armstrong, A. O., Armstrong, A. J., Bennett, M. B., Richardson, A. J., Townsend, K. A., & Dudgeon, C. L. (2019). Photographic identification and citizen science combine to reveal long distance movements of individual reef manta rays *Mobula alfredi* along Australia's east coast. *Marine Biodiversity Records*, *12*(1), 10–15. https://doi.org/10.1186/s41200-019-0173-6

Armstrong, A. O., Armstrong, A. J., Jaine, F. R. A., Couturier, L. I. E., Fiora, K., Uribe-Palomino, J., Weeks, S. J., Townsend, K. A., Bennett, M. B., & Richardson, A. J. (2016). Prey density threshold and tidal influence on reef manta ray foraging at an aggregation site on the Great Barrier Reef. *PLoS ONE*, *11*(5), 1–18. https://doi.org/10.1371/journal.pone.0153393

Australian Government Bureau of Meteorology (2012) Record-breaking La Niña events: An analysis of the La Niña life cycle and the impacts and significance of the 2010–11 and 2011–12 La Niña events in Australia, *Bureau of Meteorology*, Melbourne, [accessed 4th September 2022]

Bullock, R., Ralph, G., Stump, E., Al Abdali, F., Al Asfoor, J., Al Buwaiqi, B., Al Kindi, A., Ambuali, A., Birge, T., Borsa, P., Dario, F. Di, Everett, B., Fennessy, S., Fonseca, C., Gorman, C., Govender, A., Ho, H., Holleman, W., Jiddawi, N., … Carpenter, K. (2021). *The conservation status of marine biodiversity of the Western Indian Ocean*, IUCN, Gland, Switzerland.

Burgess, K. B., Couturier, L. I. E., Marshall, A. D., Richardson, A. J., Weeks, S. J., & Bennett, M. B. (2016). Manta birostris, predator of the deep? Insight into the diet of the giant manta ray through stable isotope analysis. *Royal Society Open Science*, *3*(11). https://doi.org/10.1098/rsos.160717

Cai, W., Santoso, A., Wang, G., Weller, E., Wu, L., Ashok, K., Masumoto, Y., & Yamagata, T. (2014). Increased frequency of extreme Indian ocean dipole events due to greenhouse warming. *Nature*, *510*(7504), 254–258. https://doi.org/10.1038/nature13327

Carlisle, A. B., Kim, S. L., Semmens, B. X., Madigan, D. J., Jorgensen, S. J., Perle, C. R., Anderson, S. D., Chapple, T. K., Kanive, P. E., & Block, B. A. (2012). Using stable isotope analysis to understand the migration and trophic ecology of northeastern Pacific white sharks (Carcharodon carcharias). *PLoS ONE*, *7*(2). https://doi.org/10.1371/journal.pone.0030492

Carlisle, A. B., Litvin, S. Y., Madigan, D. J., Lyons, K., Bigman, J. S., Ibarra, M., & Bizzarro, J. J. (2017). Interactive effects of urea and lipid content confound stable isotope analysis in elasmobranch fishes. *Canadian Journal of Fisheries and Aquatic Sciences*, *74*(3), 419–428. https://doi.org/10.1139/cjfas-2015-0584

Carr, P. (2015). Birds of the British Indian Ocean Territory Chagos Archipelago, central Indian Ocean. *Indian BIRDS*, Young *10*(3–4), 57–70.

Carr, P., Trevail, A. M., Koldewey, H. J., Sherley, R. B., Wilkinson, T., Wood, H., & Votier, S. C. (2022)

Marine Important Bird and Biodiversity Areas in the Chagos Archipelago. *Bird Conservation International*, 1–8. https://doi.org/10.1017/s0959270922000247

Chin, A., Kyne, P. M., Walker, T. I., & McAuley, R. B. (2010). An integrated risk assessment for climate change: Analysing the vulnerability of sharks and rays on Australia's Great Barrier Reef. *Global Change Biology*, *16*(7), 1936–1953. https://doi.org/10.1111/j.1365-2486.2009.02128.x

Collins, C., Nuno, A., Broderick, A., Curnick, D. J., de Vos, A., Franklin, T., Jacoby, D. M. P., Mees, C., Moir-Clark, J., Pearce, J., & Letessier, T. B. (2021). Understanding Persistent Non-compliance in a Remote, Large-Scale Marine Protected Area. *Frontiers in Marine Science*, *8*(May), 1–13. https://doi.org/10.3389/fmars.2021.650276

Couturier, L. I.E., Marshall, A. D., Jaine, F. R. A., Kashiwagi, T., Pierce, S. J., Townsend, K. A., Weeks, S. J., Bennett, M. B., & Richardson, A. J. (2012). Biology, ecology and conservation of the Mobulidae. *Journal of Fish Biology*, *80*(5), 1075–1119. https://doi.org/10.1111/j.1095-8649.2012.03264.x

Couturier, L. I.E., Rohner, C. A., Richardson, A. J., Marshall, A. D., Jaine, F. R. A., Bennett, M. B., Townsend, K. A., Weeks, S. J., & Nichols, P. D. (2013). Stable Isotope and Signature Fatty Acid Analyses Suggest Reef Manta Rays Feed on Demersal Zooplankton. *PLoS ONE*, *8*(10). https://doi.org/10.1371/journal.pone.0077152

Croll, D. A., Dewar, H., Dulvy, N. K., Fernando, D., Francis, M. P., Galván-Magaña, F., Hall, M., Heinrichs, S., Marshall, A., Mccauley, D., Newton, K. M., Notarbartolo-Di-Sciara, G., O'Malley, M., O'Sullivan, J., Poortvliet, M., Roman, M., Stevens, G., Tershy, B. R., & White, W. T. (2016). Vulnerabilities and fisheries impacts: the uncertain future of manta and devil rays. *Aquatic Conservation: Marine and Freshwater Ecosystems*, *26*(3), 562–575. https://doi.org/10.1002/aqc.2591

Daly, R., Froneman, P. W., & Smale, M. J. (2013). Comparative Feeding Ecology of Bull Sharks (Carcharhinus leucas) in the Coastal Waters of the Southwest Indian Ocean Inferred from Stable Isotope Analysis. *PLoS ONE*, *8*(10), 1–11. https://doi.org/10.1371/journal.pone.0078229

DeNiro, M. J., & Epstein, S. (1977). Mechanism of carbon isotope fractionation associated with lipid synthesis. *Science*, *197*(4300), 261–263. https://doi.org/10.1126/science.327543

Dilmahamod, A. F., Hermes, J. C., & Reason, C. J. C. (2016). Chlorophyll-a variability in the Seychelles-Chagos Thermocline Ridge: Analysis of a coupled biophysical model. *Journal of Marine Systems*, *154*, 220–232. https://doi.org/10.1016/j.jmarsys.2015.10.011

Dulvy, N. K., Fowler, S. L., Musick, J. A., Cavanagh, R. D., Kyne, P. M., Harrison, L. R., Carlson, J. K., Davidson, L. N., Fordham, S. V, Francis, M. P., Pollock, C. M., Simpfendorfer, C. A., Burgess, G. H., Carpenter, K. E., Compagno, L. J., Ebert, D. A., Gibson, C., Heupel, M. R., Livingstone, S. R., … White, W. T. (2014). Extinction risk and conservation of the world's sharks and rays. *ELife*, *3*, 1–34. https://doi.org/10.7554/elife.00590

Dulvy, N. K., Simpfendorfer, C. A., Davidson, L. N. K., Fordham, S. V., Bräutigam, A., Sant, G., & Welch, D. J. (2017). Challenges and Priorities in Shark and Ray Conservation. *Current Biology*, *27*(11), R565–R572. https://doi.org/10.1016/j.cub.2017.04.038

Dulvy, N. K., Pacoureau, N., Rigby, C. L., Pollom, R. A., Jabado, R. W., Ebert, D. A., Finucci, B., Pollock, C. M., Cheok, J., Derrick, D. H., Herman, K. B., Sherman, C. S., VanderWright, W. J., Lawson, J. M., Walls, R. H. L., Carlson, J. K., Charvet, P., Bineesh, K. K., Fernando, D., … Simpfendorfer, C. A. (2021). Overfishing drives over one-third of all sharks and rays toward a global extinction crisis. *Current Biology*, *31*(21), 4773-4787.e8. https://doi.org/10.1016/j.cub.2021.08.062

Fernando, D., & Stewart, J. D. (2021). High bycatch rates of manta and devil rays in the "small-scale" artisanal fisheries of Sri Lanka. *PeerJ*, *9*, 1–35. https://doi.org/10.7717/peerj.11994

Ferretti, F., Curnick, D., Liu, K., Romanov, E. V., & Block, B. A. (2018). Shark baselines and the conservation role of remote coral reef ecosystems. *Science Advances*, *4*(3).

https://doi.org/10.1126/sciadv.aaq0333

Fischer, W., & Bianchi, G., eds. (1984) FAO species identification sheets for fishery purposes. Western Indian Ocean (Fishing Area 51). Vol. 1-6, *FAO,* Rome.

Folch, J., Lees, M., & Sloane Stanley, G. H. (1957) A simple method for the isolation and purification of total lipides from animal tissues. *Journal of Biological Chemistry, 226* (1), 497-509, https://doi.org/10.1016/S0021-9258(18)64849-5

France, R. L. (1995) Carbon-13 enrichment in benthic compared to planktonic algae: foodweb implications. *Marine Ecology Progress Series, 124,* 307-312, doi:10.3354/meps124307

Fry, B. (2006) Stable Isotope Ecology. *Springer,* New York.

Gallagher, A. J., Kyne, P. M., & Hammerschlag, N. (2012). Ecological risk assessment and its application to elasmobranch conservation and management. *Journal of Fish Biology*, *80*(5), 1727–1748. https://doi.org/10.1111/j.1095-8649.2012.03235.x

Graham, N. A. J., Wilson, S. K., Carr, P., Hoey, A. S., Jennings, S., & MacNeil, M. A. (2018). Seabirds enhance coral reef productivity and functioning in the absence of invasive rats. *Nature*, *559*(7713), 250–253. https://doi.org/10.1038/s41586-018-0202-3

Harper, G. A., Carr, P., & Pitman, H. (2019) Eradicating black rats from the Chagos – working towards the whole archipelago *in Island invasives: scaling up to meet the challenge,* Veitch, C.R., Clout, M.N., Martin, A.R., Russell, J.C., & West, C.J. (eds), pp 26-30, IUCN, Switzerland

Harris, J. L. (2019) Reef manta rays, *Mobula alfredi*, of the Chagos Archipelago: Habitat use and the effectiveness of the region's marine protected area. MRes Thesis. University of Plymouth.

Harris, J. L., Hosegood, P., Robinson, E., Embling, C. B., Hilbourne, S., & Stevens, G. M. W. (2021). Fine-scale oceanographic drivers of reef manta ray (Mobula alfredi) visitation patterns at a feeding aggregation site. *Ecology and Evolution*, *11*(9), 4588–4604. https://doi.org/10.1002/ece3.7357

Harris, J. L., McGregor, P. K., Oates, Y., & Stevens, G. M. W. (2020). Gone with the wind: Seasonal distribution and habitat use by the reef manta ray (Mobula alfredi) in the Maldives, implications for conservation. *Aquatic Conservation: Marine and Freshwater Ecosystems*, *30*(8), 1649–1664. https://doi.org/10.1002/aqc.3350

Hays, G. C., Koldewey, H. J., Andrzejaczek, S., Attrill, M. J., Barley, S., Bayley, D. T. I., Benkwitt, C. E., Block, B., Schallert, R. J., Carlisle, A. B., Carr, P., Chapple, T. K., Collins, C., Diaz, C., Dunn, N., Dunbar, R. B., Eager, D. S., Engel, J., Embling, C. B., … Curnick, D. J. (2020). A review of a decade of lessons from one of the world's largest MPAs: conservation gains and key challenges. *Marine Biology*, *167*(11), 1–22. https://doi.org/10.1007/s00227-020-03776-w

Huang, J. L., Leroy, E. C., Truong, G., & Rogers, T. L. (2022). Changes of Oceanic Conditions Drive Chagos Whale Migration Patterns in the Central Indian Ocean. *Frontiers in Marine Science*, *9*(June), 1–14. https://doi.org/10.3389/fmars.2022.843875

Hussey, N. E., Olin, J. A., Kinney, M. J., McMeans, B. C., & Fisk, A. T. (2012a). Lipid extraction effects on stable isotope values (δ 13C and δ 15N) of elasmobranch muscle tissue. *Journal of Experimental Marine Biology and Ecology*, *434–435*, 7–15. https://doi.org/10.1016/j.jembe.2012.07.012

Hussey, N. E., MacNeil, M. A., Olin, J. A., McMeans, B. C., Kinney, M. J., Chapman, D. D., & Fisk, A. T. (2012b). Stable isotopes and elasmobranchs: Tissue types, methods, applications and assumptions. *Journal of Fish Biology*, *80*(5), 1449–1484. https://doi.org/10.1111/j.1095-8649.2012.03251.x

Jacoby, D. M. P., Ferretti, F., Freeman, R., Carlisle, A. B., Chapple, T. K., Curnick, D. J., Dale, J. J., Schallert, R. J., Tickler, D., & Block, B. A. (2020) Shark movement strategies influence poaching risk and can guide

enforcement decisions in a large, remote marine protected area. *Journal of Applied Ecology, 57,* 1782-1792, https://doi.org/10.1111/1365-2664.13654

Jones, H. P., Tershy, B. R., Zavaleta, E. S., Croll, D. A., Keitt, B. S., Finkelstein, M. E., & Howald, G. R. (2008). Severity of the effects of invasive rats on seabirds: A global review. *Conservation Biology*, *22*(1), 16–26. https://doi.org/10.1111/j.1523-1739.2007.00859.x

Jorgensen, S., Micheli, F., White, T., Van Houtan, K., Alfaro-Shigueto, J., Andrzejaczek, S., Arnoldi, N., Baum, J., Block, B., Britten, G., Butner, C., Caballero, S., Cardeñosa, D., Chapple, T., Clarke, S., Cortés, E., Dulvy, N., Fowler, S., Gallagher, A., … Ferretti, F. (2022). Emergent research and priorities for shark and ray conservation. *Endangered Species Research*, *47*(March), 171–203. https://doi.org/10.3354/esr01169

Kim, S. L., & Koch, P. (2012). Methods to collect , preserve , and prepare elasmobranch tissues for stable isotope analysis Related papers tissues for stable isotope analysis. *Environmental Biology of Fishes*, *95*, 53–63. https://doi.org/10.1007/s10641-011-9860-9

Knip, D. M., Heupel, M. R., & Simpfendorfer, C. A. (2010). Sharks in nearshore environments: Models, importance, and consequences. *Marine Ecology Progress Series*, *402*, 1–11. https://doi.org/10.3354/meps08498

Lawson, J. M., Fordham, S. V., O'Malley, M. P., Davidson, L. N. K., Walls, R. H. L., Heupel, M. R., Stevens, G., Fernando, D., Budziak, A., Simpfendorfer, C. A., Ender, I., Francis, M. P., di Sciara, G. N., & Dulvy, N. K. (2017). Sympathy for the devil: A conservation strategy for devil and manta rays. *PeerJ*, *2017*(3). https://doi.org/10.7717/peerj.3027

Lee, E., Kim, C., & Na, H. (2022). Suppressed Upwelling Events in the Seychelles–Chagos Thermocline Ridge of the Southwestern Tropical Indian Ocean. *Ocean Science Journal*, *57*(2), 305–313. https://doi.org/10.1007/s12601-022-00075-x

Li, Y., Zhang, Y., Hussey, N. E., & Dai, X. (2016). Urea and lipid extraction treatment effects on δ15N and δ13C values in pelagic sharks. *Rapid Communications in Mass Spectrometry*, *30*(1), 1–8. https://doi.org/10.1002/rcm.7396

MacNeil, M. A., Chapman, D. D., Heupel, M., Simpfendorfer, C. A., Heithaus, M., Meekan, M., Harvey, E., Goetze, J., Kiszka, J., Bond, M. E., Currey-Randall, L. M., Speed, C. W., Sherman, C. S., Rees, M. J., Udyawer, V., Flowers, K. I., Clementi, G., Valentin-Albanese, J., Gorham, T., … Cinner, J. E. (2020). Global status and conservation potential of reef sharks. *Nature*, *583*(7818), 801–806. https://doi.org/10.1038/s41586-020-2519-y

MacNeil, M. A., Skomal, G. B., & Fisk, A. T. (2005). Stable isotopes from multiple tissues reveal diet switching in sharks. *Marine Ecology Progress Series*, *302*, 199–206. https://doi.org/10.3354/meps302199

Marcus, L., Virtue, P., Nichols, P. D., Ferreira, L. C., Pethybridge, H., & Meekan, M. G. (2019). Stable Isotope Analysis of Dermis and the Foraging Behavior of Whale Sharks at Ningaloo Reef, Western Australia. *Frontiers in Marine Science*, *6*(September), 1–11. https://doi.org/10.3389/fmars.2019.00546

Marcus, L., Virtue, P., Nichols, P. D., Meekan, M. G., & Pethybridge, H. (2017). Effects of sample treatment on the analysis of stable isotopes of carbon and nitrogen in zooplankton, micronekton and a filter-feeding shark. *Marine Biology*, *164*(6), 1–12. https://doi.org/10.1007/s00227-017-3153-6

Marine Conservation Institute (2021) The Atlas of Marine Protection, available at: http://mpatlas.org [Accessed: 8 September 2022]

Marshall, A. D., Barreto, R., Fernando, D., & Francis, M. (2019). *Mobula alfredi-Reef Manta Ray. The IUCN Red List of Threatened Species 2019* https://doi.org/10.2305/IUCN.UK.2019-3.RLTS.T195459A68632178.en

McCauley, D. J., Desalles, P. A., Young, H. S., Dunbar, R. B., Dirzo, R., Mills, M. M., & Micheli, F. (2012).

From wing to wing: The persistence of long ecological interaction chains in less-disturbed ecosystems. *Scientific Reports*, *2* (409). https://doi.org/10.1038/srep00409

Meekan, M. G., Fuiman, L. A., Davis, R., Berger, Y., & Thums, M. (2015). Swimming strategy and body plan of the world's largest fish: Implications for foraging efficiency and thermoregulation. *Frontiers in Marine Science*, *2*(SEP), 1–8. https://doi.org/10.3389/fmars.2015.00064

Munroe, S. E. M., Meyer, L., & Heithaus, M. R. (2020) Dietary Biomarkers in Shark Foraging and Movement Ecology *in Shark Research: Emerging Technologies and Applications for the Field and Laboratory,* Carrier, J.C., Heithaus, M.R., & Simpfendorfer, C.A. (eds), CRC Press, Boca Raton.

NOAA. What is upwelling? *National Ocean Service* website, available at: https://oceanservice.noaa.gov/facts/upwelling.html, [accessed 4th September 2022]

Parnell, A. (2016) simmr: A Stable Isotope Mixing Model. R Package version 0.3. See https://cran.r-project.org/web/packages/simmr/simmr.pdf

Peel, L. R., Daly, R., Keating Daly, C. A., Stevens, G. M. W., Collin, S. P., & Meekan, M. G. (2019). Stable isotope analyses reveal unique trophic role of reef manta rays (Mobula alfredi) at a remote coral reef. *Royal Society Open Science*, *6*(9). https://doi.org/10.1098/rsos.190599

Peel, L. R., Stevens, G. M. W., Daly, R., Keating Daly, C. A., Collin, S. P., Nogués, J., & Meekan, M. G. (2020). Regional Movements of Reef Manta Rays (Mobula alfredi) in Seychelles Waters. *Frontiers in Marine Science*, *7*. https://doi.org/10.3389/fmars.2020.00558

Peterson, B. J, & Fry, B. (1987). Stable isotopes in ecosystem studies. *Annual Review of Ecology and Systematics, 18*, 293-320, https://doi.org/10.1146/annurev.es.18.110187.001453

Post, D. M. (2002) Using stable isotopes to estimate trophic position: models, methods and assumptions. *Ecology, 83*(3), 703-718, https://doi.org/10.1890/0012-9658(2002)083[0703:USITET]2.0.CO;2

Rocliffe, S., Peabody, S., Samoilys, M., & Hawkins, J. P. (2014). Towards a network of locally managed marine areas (LMMAs) in the Western Indian Ocean. *PLoS ONE*, *9*(7). https://doi.org/10.1371/journal.pone.0103000

Rohner, C. A., Pierce, S. J., Marshall, A. D., Weeks, S. J., Bennett, M. B., & Richardson, A. J. (2013). Trends in sightings and environmental influences on a coastal aggregation of manta rays and whale sharks. *Marine Ecology Progress Series*, *482*, 153–168. https://doi.org/10.3354/meps10290

Saji, N., Goswami, B., Vinayachandran, P., & Yamagata, T. (1999). A dipole mode in the Tropical Ocean. *Nature*, *401*(6751), 360–363. https://doi.org/10.1038/43854

Seitz, J. C., & Poulakis, G. R. (2006). Anthropogenic effects on the smalltooth sawfish (Pristis pectinata) in the United States. *Marine Pollution Bulletin*, *52*(11), 1533–1540. https://doi.org/10.1016/j.marpolbul.2006.07.016

Setyawan, E., Sianipar, A. B., Erdmann, M. V., Fischer, A. M., Haddy, J. A., Beale, C. S., Lewis, S. A., & Mambrasar, R. (2018). Site fidelity and movement patterns of reef manta rays *(Mobula alfredi*: Mobulidae) using passive acoustic telemetry in northern raja Ampat, Indonesia. *Nature Conservation Research*, *3*(4), 17–31. https://doi.org/10.24189/ncr.2018.043

Sharples, J., Moore, C. M., Rippeth, T. P., Holligan, P. M., Hydes, D. J., Fisher, N. R., & Simpson, J. H. (2001). Phytoplankton distribution and survival in the thermocline. *Limnology and Oceanography*, *46*(3), 486–496. https://doi.org/10.4319/lo.2001.46.3.0486

Shatova, O., Wing, S. R., Gault-Ringold, M., Wing, L., & Hoffmann, L. J. (2016). Seabird guano enhances phytoplankton production in the Southern Ocean. *Journal of Experimental Marine Biology and Ecology*, *483*, 74–87. https://doi.org/10.1016/j.jembe.2016.07.004

Sheppard, C. R. C., Ateweberhan, M., Bowen, B. W., Carr, P., Chen, C. A., Clubbe, C., Craig, M. T., Ebinghaus, R., Eble, J., Fitzsimmons, N., Gaither, M. R., Gan, C. H., Gollock, M., Guzman, N., Graham, N. A. J., Harris, A., Jones, R., Keshavmurthy, S., Koldewey, H., … Yesson, C. (2012). Reefs and islands of the Chagos Archipelago, Indian Ocean: Why it is the world's largest no-take marine protected area. *Aquatic Conservation: Marine and Freshwater Ecosystems*, *22*(2), 232–261. https://doi.org/10.1002/aqc.1248

Shi, W., & Wang, M. (2021). A biological Indian Ocean Dipole event in 2019. *Scientific Reports*, *11*(1), 1–8. https://doi.org/10.1038/s41598-021-81410-5

Shiffman, D. S., Gallagher, A. J., Boyle, M. D., Hammerschlag-Peyer, C. M., & Hammerschlag, N. (2012). Stable isotope analysis as a tool for elasmobranch conservation research: A primer for non-specialists. In *Marine and Freshwater Research*, *63*(7)*,* 635–643. https://doi.org/10.1071/MF11235

Shiffman, D. S., Frazier, B. S., Kucklick, J. R., Abel, D., Brandes, J., & Sancho, G. (2014). Feeding Ecology of the Sandbar Shark in South Carolina Estuaries Revealed through δ13C and δ15N Stable Isotope Analysis. *Marine and Coastal Fisheries*, *6*(1), 156–169. https://doi.org/10.1080/19425120.2014.920742

Silva, M. A., Borrell, A., Prieto, R., Gauffier, P., Bérubé, M., Palsbøl, P. J., & Colaço, A. (2019). Stable isotopes reveal winter feeding in different habitats in blue, fin and sei whales migrating through the Azores. *Royal Society Open Science*, *6*(8). https://doi.org/10.1098/rsos.181800

Stevens, G. (2016). Conservation and Population Ecology of Manta Rays in the Maldives. *PhD Thesis, University of York*.

Stevens, G., Fernando, D., Dando, M., & Notarbartolo di Sciara, G. (2018) Guide to the Manta and Devil Rays of the World. *Wild Nature Press,* Plymouth.

Stewart, J. D., Jaine, F. R. A., Armstrong, A. J., Armstrong, A. O., Bennett, M. B., Burgess, K. B., Couturier, L. I. E., Croll, D. A., Cronin, M. R., Deakos, M. H., Dudgeon, C. L., Fernando, D., Froman, N., Germanov, E. S., Hall, M. A., Hinojosa-Alvarez, S., Hosegood, J. E., Kashiwagi, T., Laglbauer, B. J. L., … Stevens, G. M. W. (2018). Research priorities to support effective Manta and Devil Ray conservation. *Frontiers in Marine Science*, *5*(SEP), 1–27. https://doi.org/10.3389/fmars.2018.00314

Strike, E. M., Harris, J. L., Ballard, K. L., Hawkins, J. P., Crockett, J., & Stevens, G. M. W. (2022). Sublethal Injuries and Physical Abnormalities in Maldives Manta Rays, *Mobula alfredi* and *Mobula birostris*. *Frontiers in Marine Science*, *9*(March), 1–19. https://doi.org/10.3389/fmars.2022.773897

Tickler, D. M., Carlisle, A. B., Chapple, T. K., Curnick, D. J., Dale, J. J., Schallert, R. J., & Block, B. A. (2019). Potential detection of illegal fishing by passive acoustic telemetry. *Animal Biotelemetry*, *7*(1), 1–11. https://doi.org/10.1186/s40317-019-0163-9

Tieszen, L. L., Boutton, T. W., Tesdahl, K. G., & Slade, N. A. (1983). Fractionation and turnover of stable carbon isotopes in animal tissues: Implications for δ13C analysis of diet. *Oecologia*, *57*(1–2), 32–37. https://doi.org/10.1007/BF00379558

Wu, M., Duvat, V. K. E., & Purkis, S. J. (2021) Multi-decadal atoll-island dynamics in the Indian Ocean Chagos Archipelago. *Global and Planetary Change, 202,* 103519. https://doi.org/10.1016/j.gloplacha.2021.103519

Zhao, S., Jin, F. F., & Stuecker, M. F. (2019). Improved Predictability of the Indian Ocean Dipole Using Seasonally Modulated ENSO Forcing Forecasts. *Geophysical Research Letters*, *46*(16), 9980–9990. https://doi.org/10.1029/2019GL084196

APPENDICES

Appendix A

Table 2: Details of *M. alfredi* individuals which were sampled for tissue biopsies.

Manta ID	Sex	Maturity	Year	Location	Tissue
CG-MA-0056	F	Juvenile	2021	Salomon	Muscle + skin
CG-MA-0213	F	Adult	2021	Peros Banhos	Muscle + skin
CG-MA-0215	F	Juvenile	2021	Salomon	Muscle + skin
CG-MA-0217	M	Adult	2021	Salomon	Muscle + skin
CG-MA-0218	F	Juvenile	2021	Salomon	Muscle + skin
CG-MA-0220	F	Juvenile	2021	Salomon	Muscle + skin
CG-MA-0221	F	Juvenile	2021	Salomon	Muscle + skin
CG-MA-0222	F	Juvenile	2021	Salomon	Muscle + skin
CG-MA-0226	F	Adult	2021	Salomon	Muscle + skin
CG-MA-0027	M	Adult	2019	Egmont	Muscle
CG-MA-0055	F	Adult	2020	Egmont	Muscle + skin
CG-MA-0084	M	Juvenile	2019	Egmont	Muscle + skin
CG-MA-0088	M	Juvenile	2019	Egmont	Muscle + skin
CG-MA-0094	F	Juvenile	2019	Egmont	Muscle + skin
CG-MA-0100	M	Adult	2020	Egmont	Muscle + skin
CG-MA-0102	F	Juvenile	2019	Egmont	Muscle + skin
CG-MA-0112	M	Juvenile	2019	Egmont	Muscle + skin
CG-MA-0113	F	Juvenile	2019	Egmont	Muscle + skin
CG-MA-0115	F	Juvenile	2019	Egmont	Muscle + skin
CG-MA-0116	F	Juvenile	2019	Egmont	Muscle + skin
CG-MA-0117	F	Juvenile	2019	Egmont	Muscle + skin
CG-MA-0121	M	Juvenile	2019	Egmont	Muscle + skin
CG-MA-0126	F	Juvenile	2019	Egmont	Muscle + skin
CG-MA-0129	M	Juvenile	2019	Egmont	Muscle + skin
CG-MA-0135	F	Juvenile	2020	Egmont	Muscle + skin
CG-MA-0141	M	Adult	2019	Egmont	Muscle + skin
CG-MA-0143	F	Juvenile	2019	Egmont	Muscle + skin
CG-MA-0149	F	Juvenile	2019	Egmont	Muscle + skin
CG-MA-0152	M	Adult	2019	Egmont	Muscle + skin
CG-MA-0153	F	Adult	2019	Egmont	Muscle + skin
CG-MA-0154	M	Adult	2019	Egmont	Muscle + skin
CG-MA-0155	M	Adult	2019	Egmont	Muscle + skin
CG-MA-0163	F	Juvenile	2020	Egmont	Muscle + skin
CG-MA-0165	F	Juvenile	2020	Egmont	Muscle + skin
CG-MA-0090	M	Adult	2021	Egmont	Muscle + skin
CG-MA-0096	M	Adult	2021	Egmont	Muscle + skin
CG-MA-0098	M	Adult	2021	Egmont	Muscle + skin
CG-MA-0231	F	Juvenile	2021	Egmont	Muscle + skin
CG-MA-0232	M	Adult	2021	Egmont	Muscle + skin
CG-MA-0235	M	Juvenile	2021	Egmont	Muscle + skin
CG-MA-0189	F	Adult	2020	Egmont	Skin

Appendix B

Table 3: Details of dietary source sampling. All plankton excluding that from Sandes were used in ANOVA analyses. All plankton and fish were used in Bayesian mixing models.

Type	**Location**	**Year**	**n**
Plankton	Egmont	2019	17
Plankton	Egmont	2020	10
Plankton	Egmont	2021	15
Plankton	GCB – Brothers	2021	5
Plankton	GCB - Nelson	2021	2
Plankton	Peros Banhos	2021	9
Plankton	Salomon	2021	11
Plankton	Sandes	2022	5
Fish	Diego Garcia	2019	31
Rainbow runner			25
Bohar snapper			4
Bluefin trevally			2

Appendix C

Isotopic signatures of *M. alfredi* muscle, *M. alfredi* skin and plankton show significant differences in $\delta^{15}N$ and $\delta^{13}C$ values.

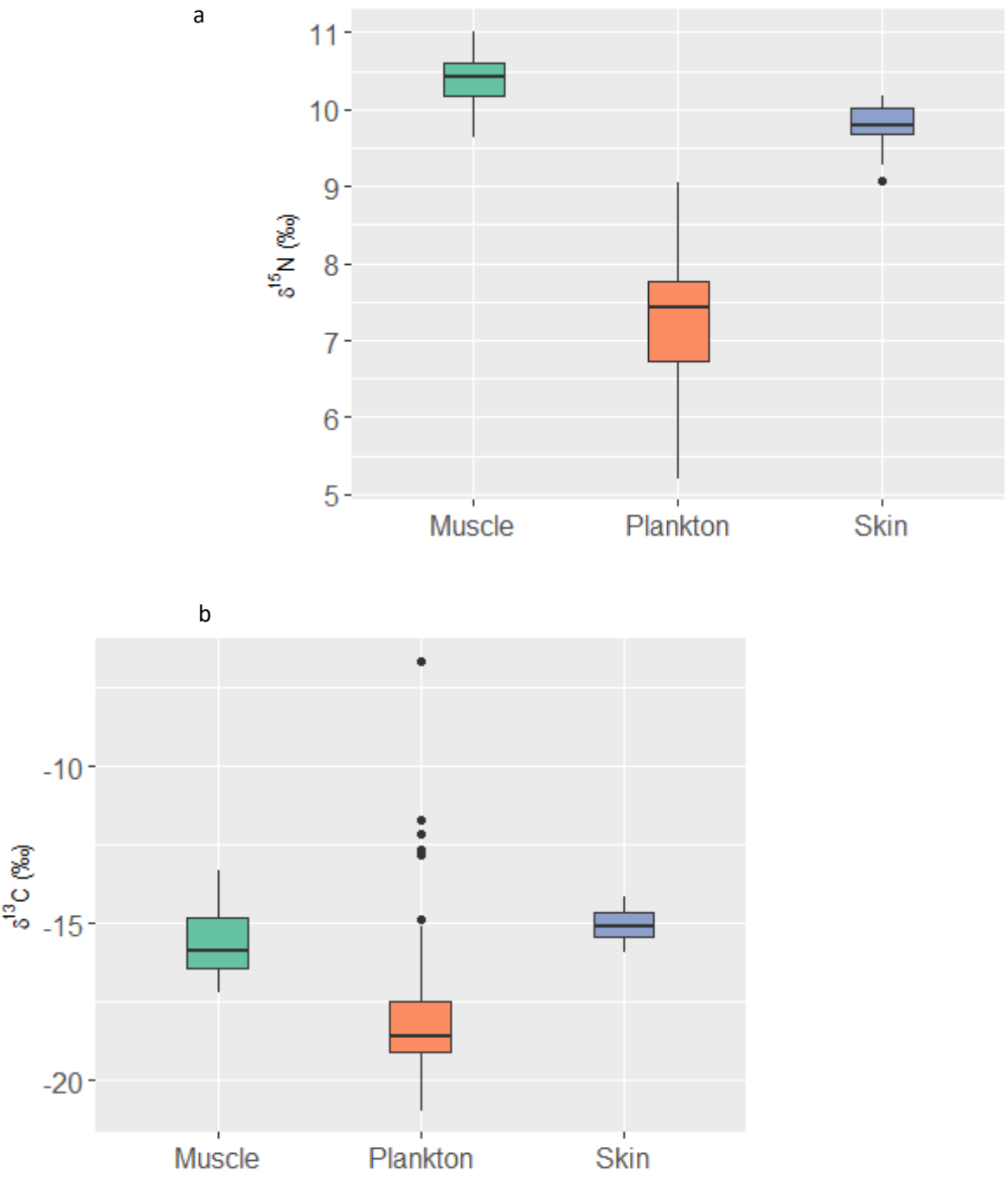

Figure 12: Boxplots of the (a) δ15N signatures and (b) $\delta^{13}C$ signatures of *M. alfredi* muscle, *M. alfredi* skin and bulk plankton. Coloured boxes encompass the interquartile range, the middle line denotes the median and the whiskers show the minimum and maximum values. Outliers are represented by circles.

Appendix D

Mobula alfredi skin showed significant depletion in $\delta^{13}C$ from individuals sampled in the south compared to those from the north (ANOVA $F_{1,38} = 9.771$, $p = 0.003$) (Figure 13).

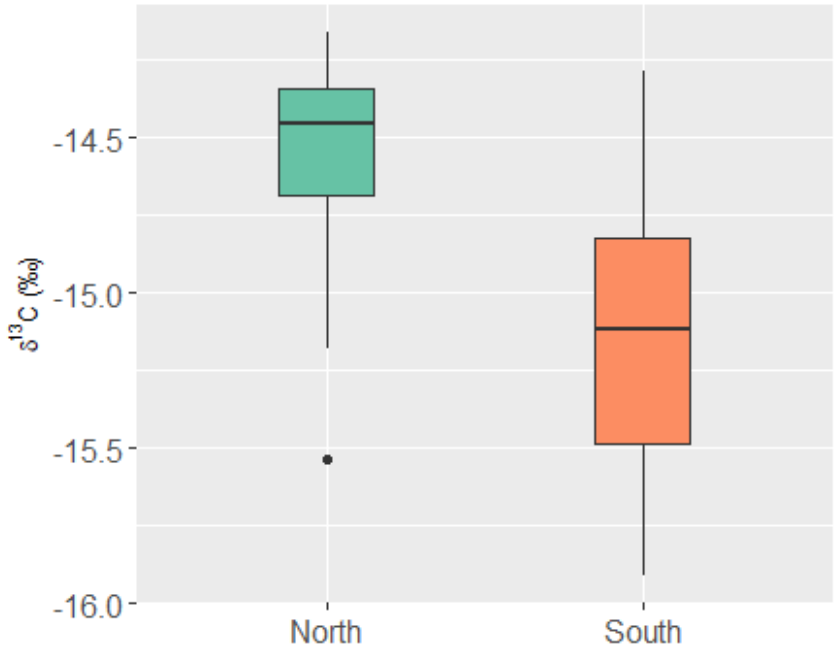

Figure 13: Boxplot of *M. alfredi* skin $\delta^{13}C$ values from *M. alfredi* sampled in the north (Peros Banhos and Salomon) and the south (Egmont) across all years. Coloured boxes encompass the interquartile range, the middle line denotes the median and the whiskers show the minimum and maximum values. Outliers are represented by circles.